The Basics of Particle Detection

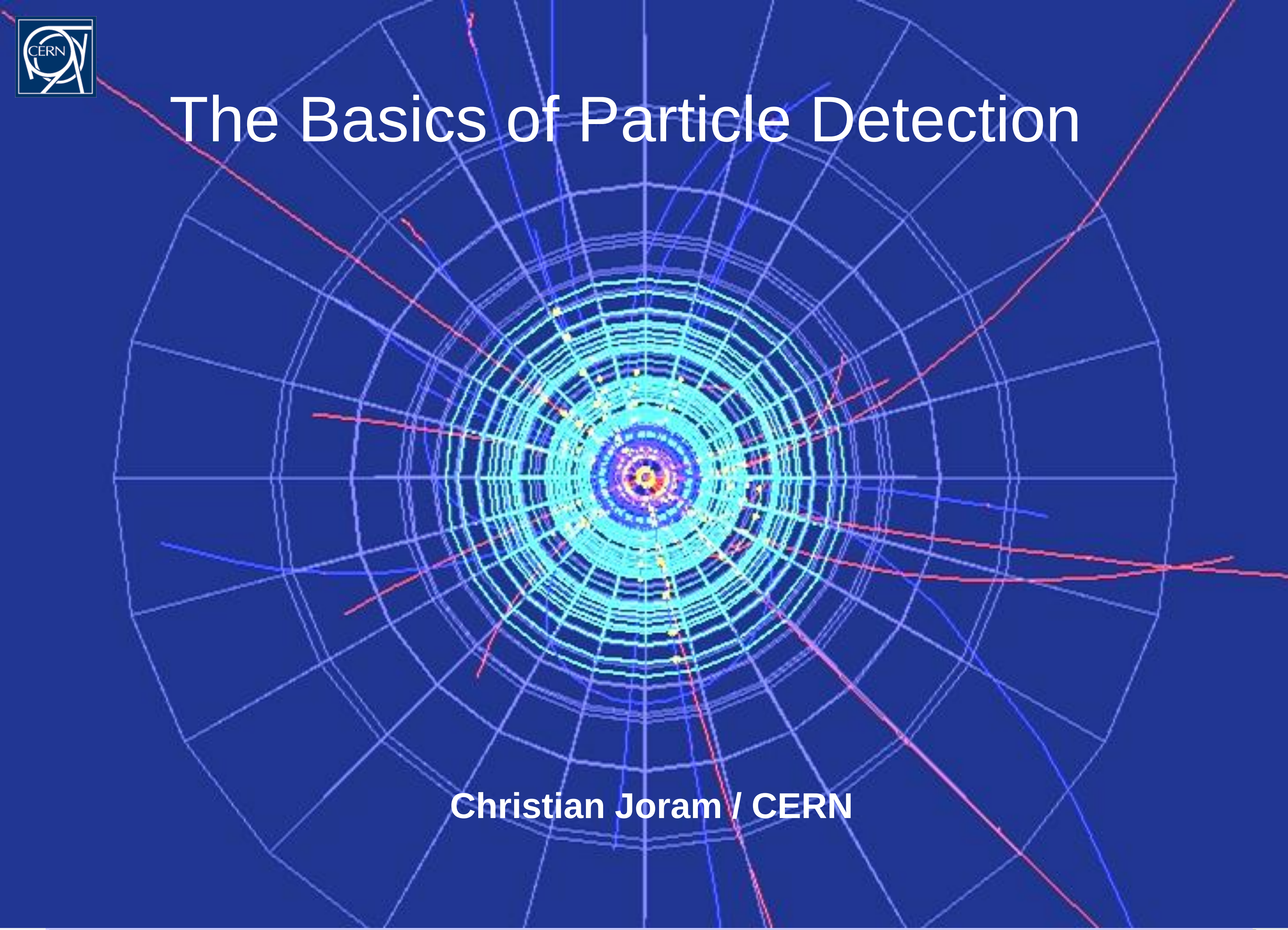

Christian Joram / CERN

Outline

- Lecture 1 – **Interaction of charged particles**
- Lecture 2 – **Gaseous and solid state tracking detectors**
  - Concept of momentum measurement
  - Gas detectors
  - Solid state (Silicon) detectors
  - More interactions of charged particles and photons
- Lecture 3 – **Calorimetry, scintillation and photodetection**

Momentum measurement

Momentum *p*

Measure the radius of curvature ρ in a magnetic field

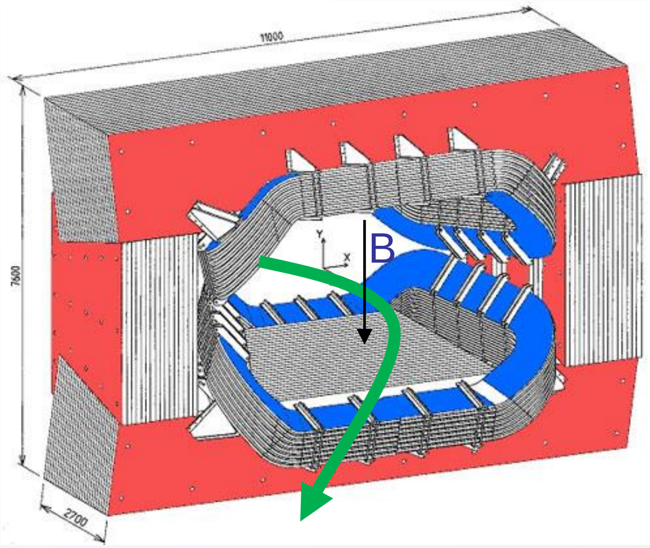

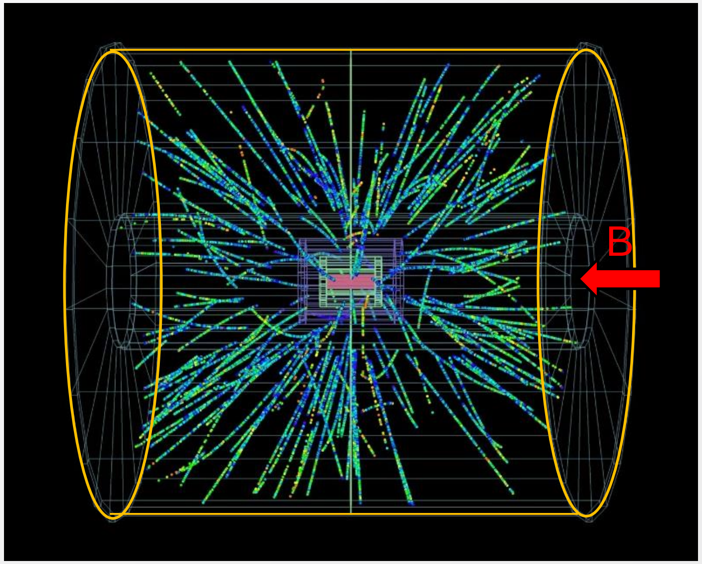

Momentum measurement (in solenoidal field)

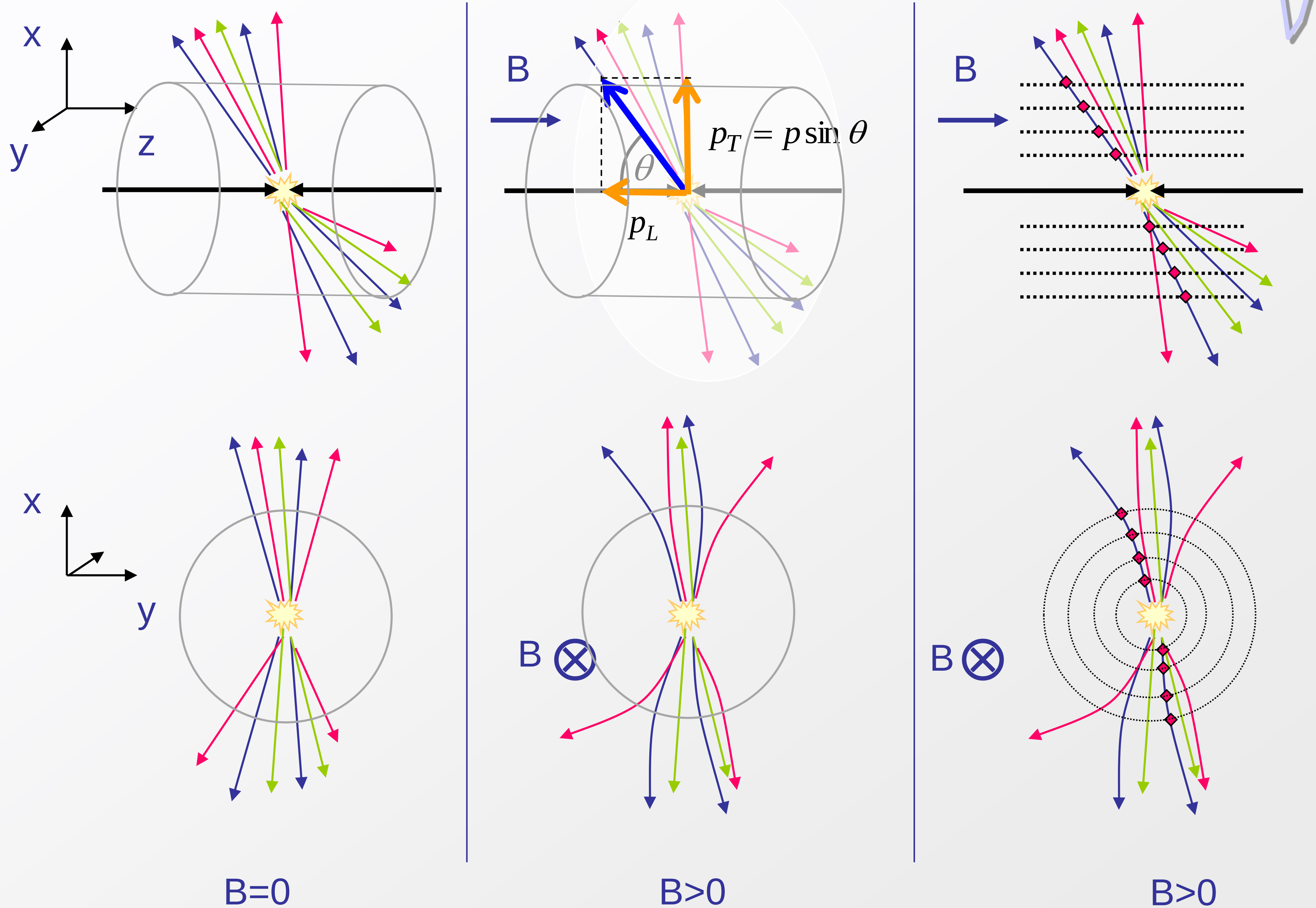

Momentum measurement

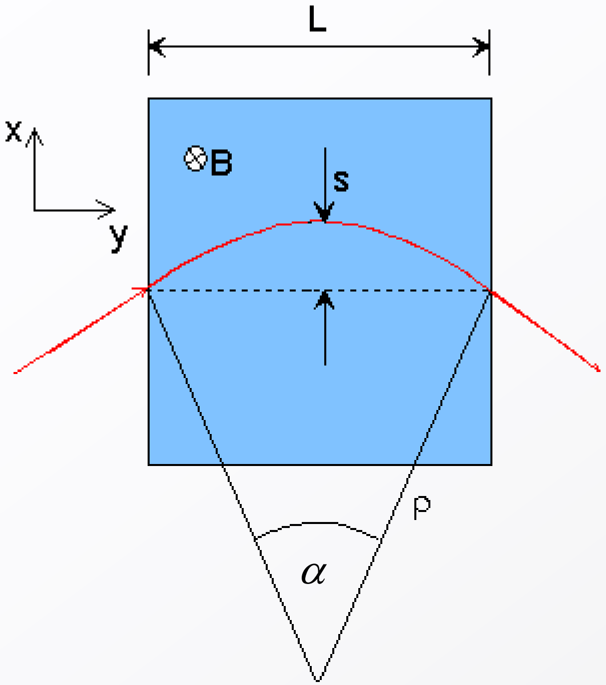

We measure only p-component transverse to B field !

$$p_T = qB\rho \quad \rightarrow \quad p_T\ (\mathrm{GeV/c}) = 0.3B\rho \quad (\mathrm{T \cdot m})$$

$$\frac{L}{2\rho} = \sin\alpha/2 \approx \alpha/2 \quad \rightarrow \quad \alpha \approx \frac{0.3L \cdot B}{p_T}$$

$$s = \rho(1-\cos\alpha/2) \approx \rho\frac{\alpha^2}{8} \approx \frac{0.3}{8}\frac{L^2 B}{p_T}$$

the sagitta s is determined by 3 measurements with error $\sigma(x)$:

$$s = x_2 - \frac{x_1 + x_3}{2} \qquad \left.\frac{\sigma(p_T)}{p_T}\right|^{meas.} = \frac{\sigma(s)}{s} = \frac{\sqrt{\frac{3}{2}}\sigma(x)}{s} = \frac{\sqrt{\frac{3}{2}}\sigma(x)\cdot 8p_T}{0.3\cdot BL^2}$$

$$\left.\frac{\sigma(p_T)}{p_T}\right|^{meas.} \propto \frac{\sigma(x)\cdot p_T}{BL^2}$$

for N equidistant measurements, one obtains (R.L. Gluckstern, NIM 24 (1963) 381)

$$\left.\frac{\sigma(p_T)}{p_T}\right|^{meas.} = \frac{\sigma(x)\cdot p_T}{0.3\cdot BL^2}\sqrt{720/(N+4)} \qquad (\text{for } N \geq \sim 10)$$

Momentum measurement

What is the contribution of multiple scattering to $\frac{\sigma(p)}{p_T}$?

remember $\frac{\sigma(p)}{p_T} \propto \sigma(x) \cdot p_T$

$\sigma(x)\big|^{MS} \propto \theta_0 \propto \frac{1}{p}$

$$\left.\frac{\sigma(p)}{p_T}\right|^{MS} = \text{constant}$$, i.e. independent of p !

More precisely: $$\left.\frac{\sigma(p)}{p_T}\right|^{MS} = 0.045 \frac{1}{B\sqrt{LX_0}}$$

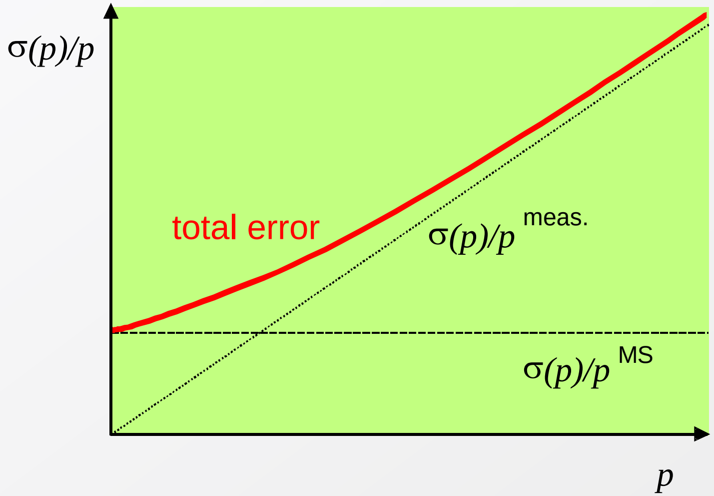

Example:

p_t = 1 GeV/c, L = 1m, B = 1 T, N = 10

$\sigma(x)$ = 200 µm: $\left.\frac{\sigma(p_T)}{p_T}\right|^{meas.} \approx 0.5\%$

Assume detector (L = 1m) to be filled with 1 atm. Argon gas (X_0 = 110m),

$\left.\frac{\sigma(p)}{p_T}\right|^{MS} \approx 0.5\%$

Optimistic, since a gas detector consists of more than just gas!

A more realistic example: CMS Silicon Tracker

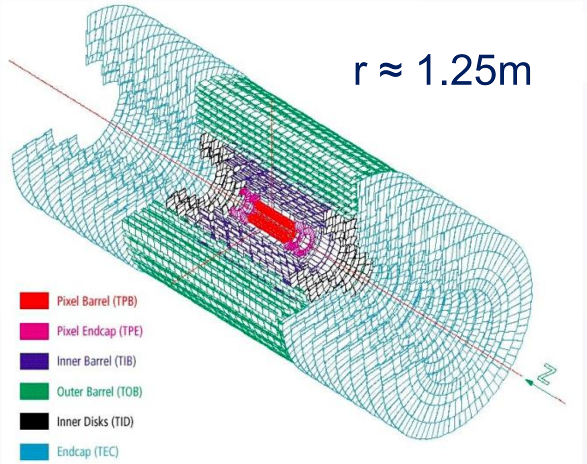

- B=3.8T, L=1.25m, average N ≈ 10 layers,
- Average resolution per layer ≈ 25μm,

$$\left.\frac{\sigma(p_T)}{p_T}\right|^{meas.} = \frac{\sigma(x)\cdot p_T}{0.3\cdot BL^2}\sqrt{720/(N+4)}$$

→ σ_p/p = 0.1 % momentum resolution (at 1 GeV)

→ σ_p/p = 10 % momentum resolution (at 1 TeV)

Material budget (Si, cables, cooling pipes, support structure…)

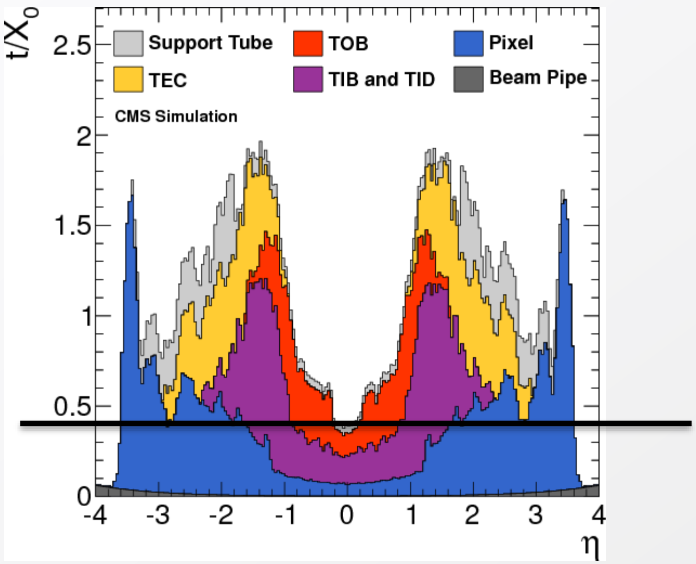

- B=3.8T, L=1.25m, t/X_0 ≈ 0.4-0.5 @ η < 1

$$\left.\frac{\sigma(p)}{p_T}\right|^{MS} = 0.045\frac{1}{B\sqrt{LX_0}} = 0.045\frac{1}{B\cdot L}\sqrt{\frac{t}{X_0}}$$

→ σ_p/p = 0.7% from multiple scattering

(η = pseudo rapidity: $\eta = -\ln(\tan\frac{\theta}{2})$)

Ionisation of Gases

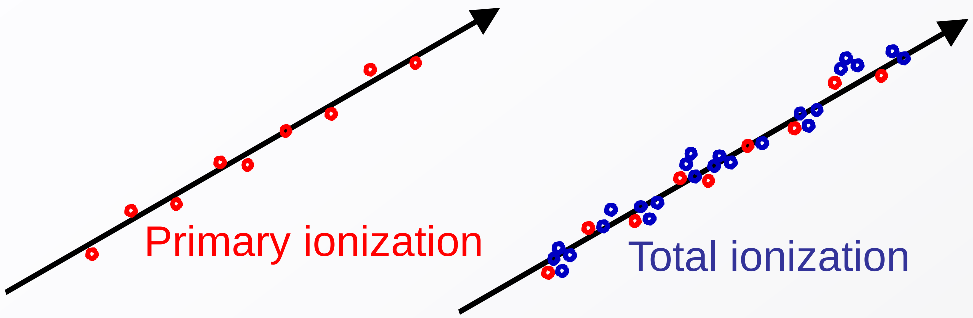

Number of primary electron/ion pairs in frequently used gases.

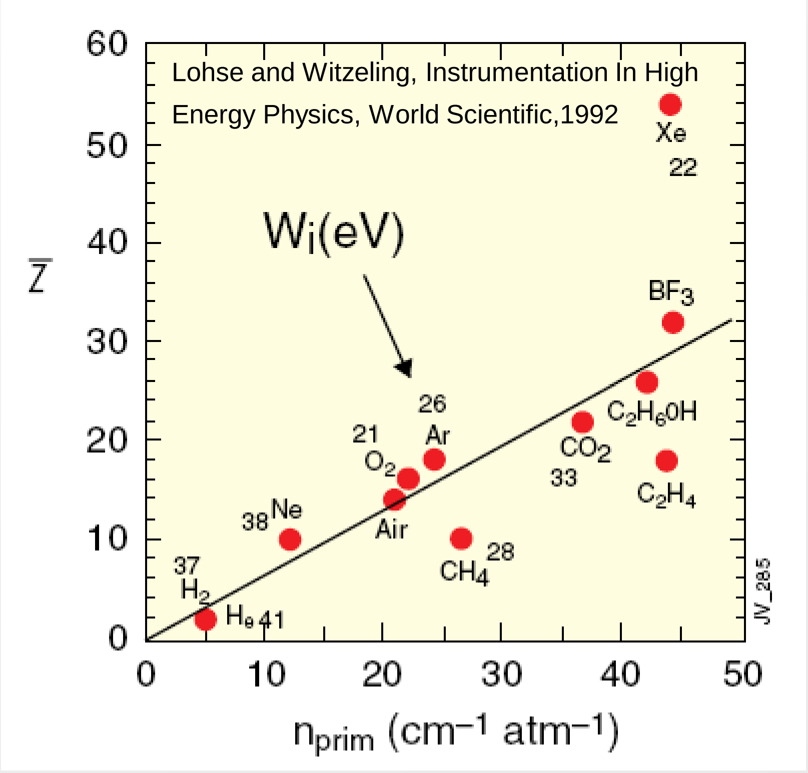

Fast charged particles ionise atoms of gas. Often, the resulting primary electrons will have enough kinetic energy to ionize other atoms.

$$n_{total} = \frac{\Delta E}{W_i} = \frac{\frac{dE}{dx}\Delta x}{W_i}$$

$$n_{total} \approx 3\ldots4 \cdot n_{primary}$$

n_{total} - number of created electron-ion pairs

Δ_E = total energy loss

W_i = effective <energy loss>/pair

Visualization of charge clusters and δ electrons

Cluster counting with a hybrid gas detector: pixel readout chip + micromegas

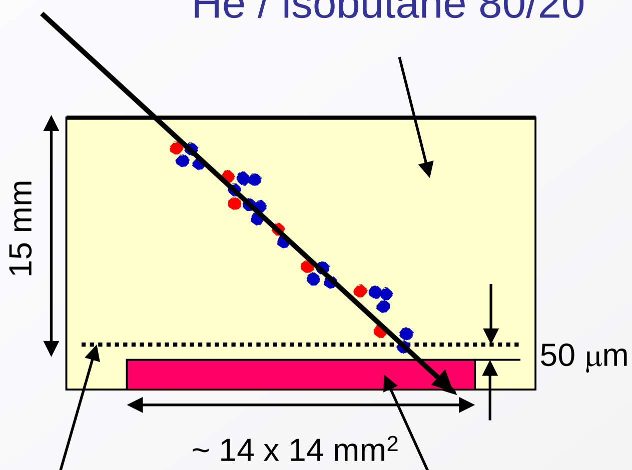

micromegas foil

Medipix chip 256 x 256 pixels, 55 x 55 μm^2, each

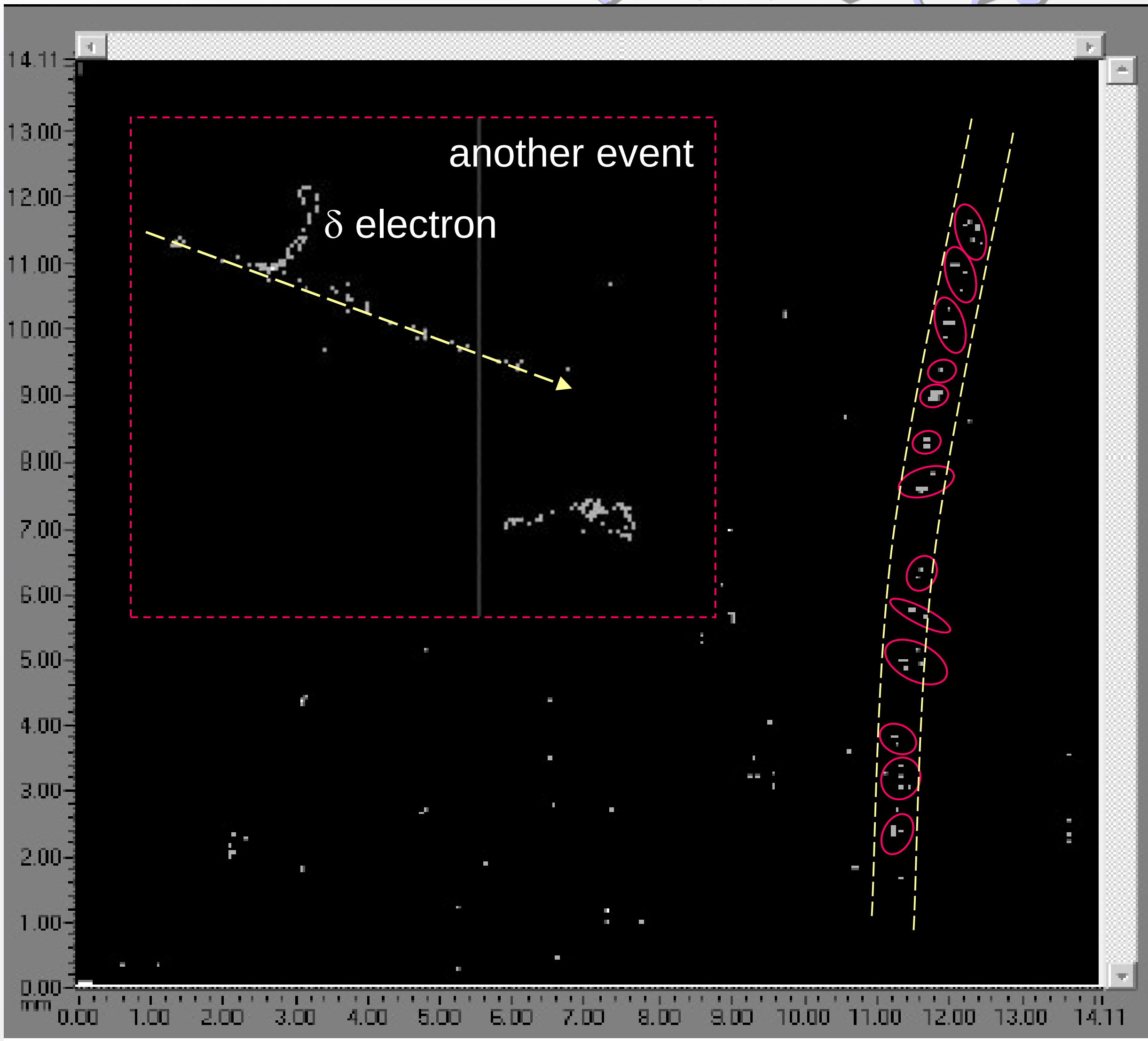

track by cosmic particle (mip): 0.52 clusters / mm, ~3 e$^-$/cluster

M. Campbell et al., NIM A 540 (2005) 295

- The actual number of primary electron/ion pairs is Poisson distributed.

$$P(m) = \frac{\mu^m e^{-\mu}}{m!}$$

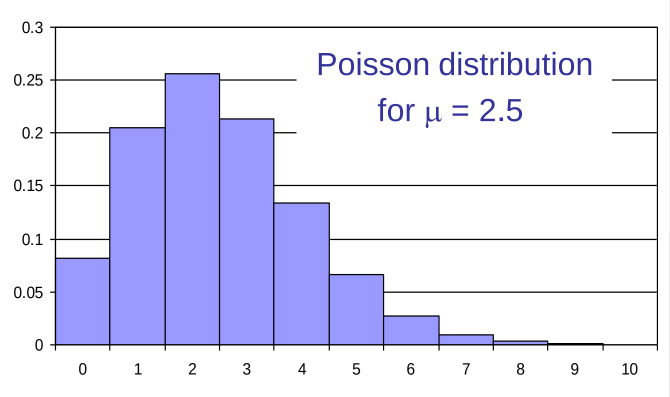

The detection efficiency is therefore limited to :

$$\varepsilon_{\text{det}} = 1 - P(0) = 1 - e^{-\mu}$$

For thin layers ε_{det} can be significantly lower than 1.

For example for 1 mm layer of Ar $n_{primary} = 2.5 \longrightarrow \varepsilon_{det} = 0.92$.

Consider a 10 mm thick Ar layer

→ $n_{primary} = 25 \longrightarrow \varepsilon_{det} = 1$

→ n_{total}= 80-100

100 electrons/ion pairs created during ionization process are not easy to detect.

Typical (equivalent) noise of an electronic amplifier ≈ 1000 e^-

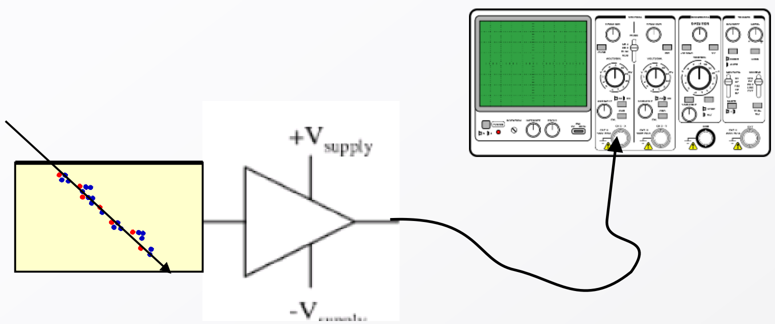

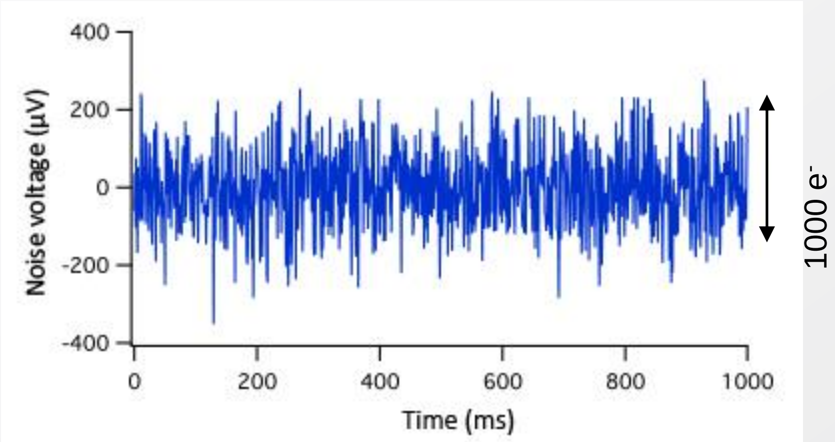

→ we will increase the number of charge carriers by **gas amplification** .

Single Wire Proportional Chamber

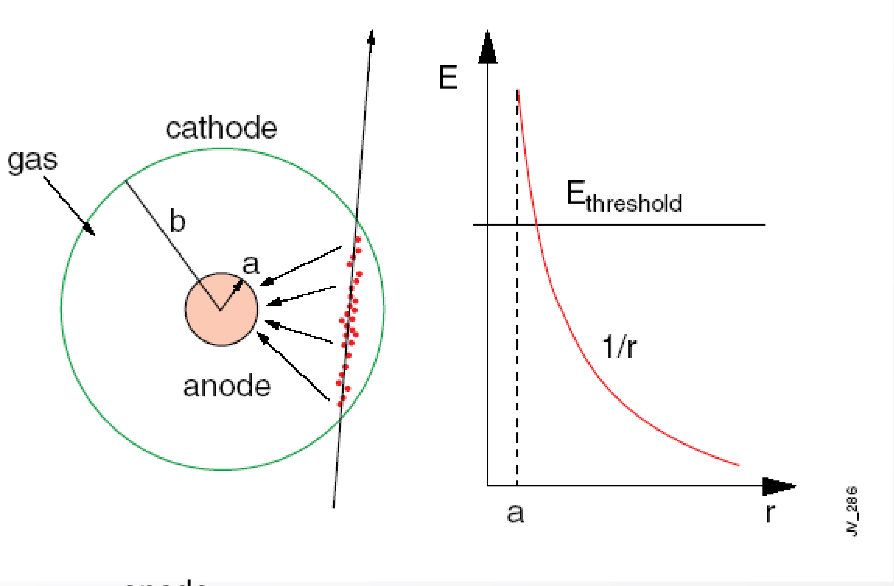

Electrons liberated by ionization drift towards the anode wire.

Electrical field close to the wire (typical wire Ø~few tens of μm) is sufficiently high for electrons (above 10 kV/cm) to gain enough energy to ionize further

→ avalanche → exponential increase of number of electron ion pairs → several thousands.

→ the signal becomes detectable.

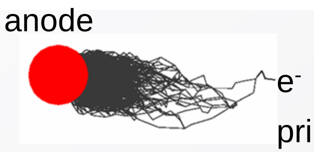

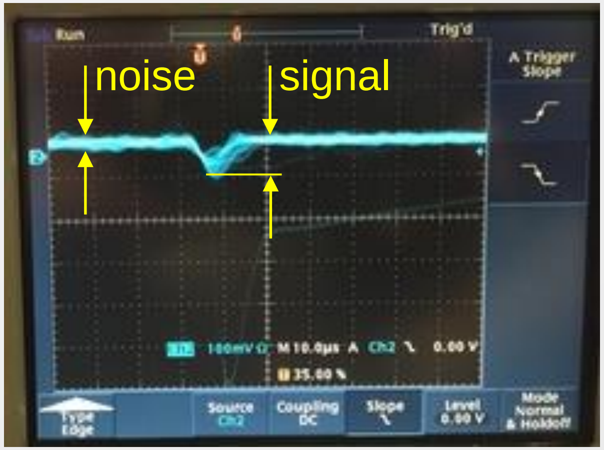

$$E(r) = \frac{CV_0}{2\pi\varepsilon_0} \cdot \frac{1}{r}$$

$$V(r) = \frac{CV_0}{2\pi\varepsilon_0} \cdot \ln\frac{r}{a}$$

C – capacitance/unit length

Multiplication of ionization is described by the first Townsend coefficient $\alpha(E)$

$$dn = n \cdot \alpha \, dx \qquad \alpha = \frac{1}{\lambda}$$

λ – mean free path

$$n = n_0 e^{\alpha(E)x} \quad \text{or} \quad n = n_0 e^{\alpha(r)x}$$

$\alpha(E)$ is determined by the excitation and ionization cross sections of the electrons in the gas.

It depends also on various and complex energy transfer mechanisms between gas molecules. There is no fundamental expression for $\alpha(E)$ → it has to be measured for every gas mixture.

$$M = \frac{n}{n_0} = \exp\left[\int_a^{r_C} \alpha(r)dr\right]$$

Amplification factor or Gain

(E/p = reduced electric field)

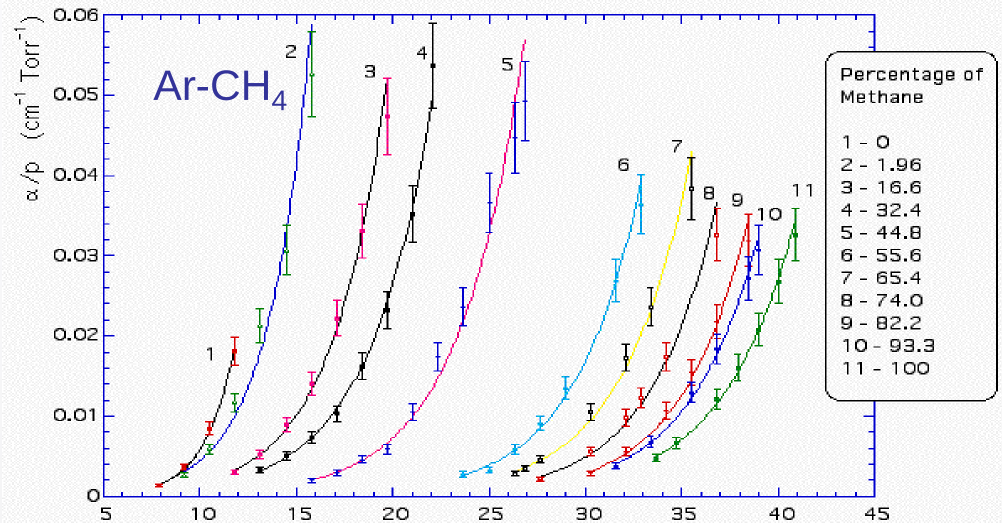

A. Sharma and F. Sauli, NIM A334(1993)420

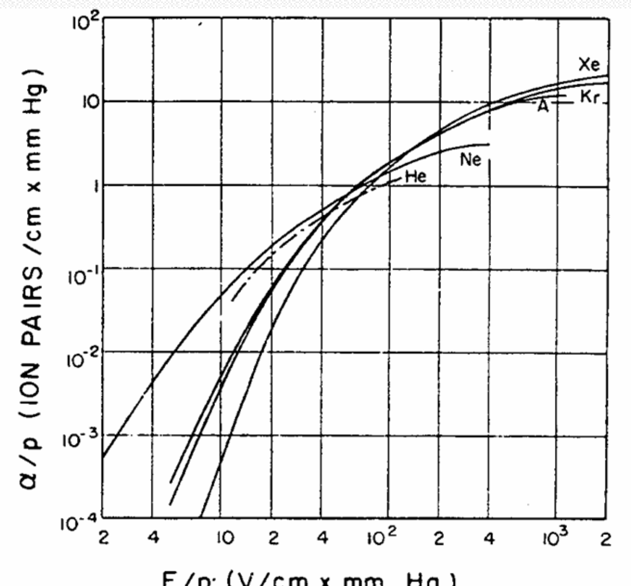

S.C. Brown, Basic data of plasma physics (MIT Press, 1959)

SWPC – Choice of Gas

In noble gases, ionization is the dominant process, but there are also excited states.

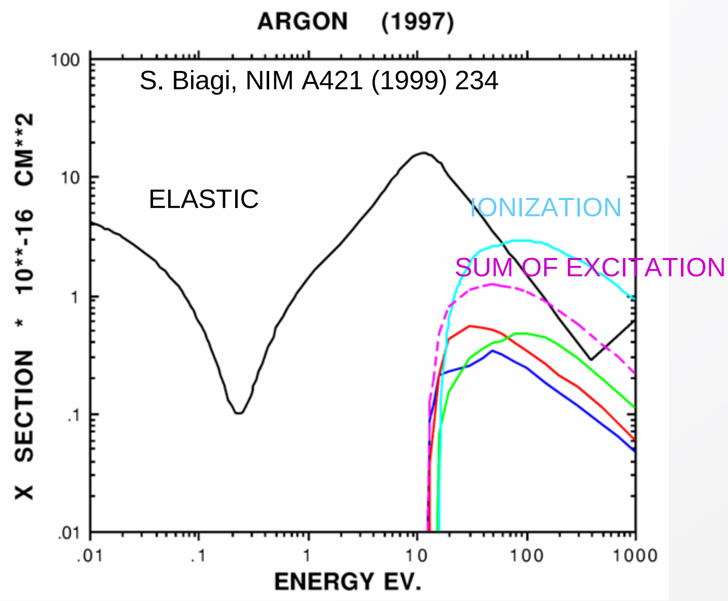

De-excitation of noble gases only via emission of photons; e.g. 11.6 eV for Ar. This is above ionization threshold of metals, e.g. Cu 7.7 eV.

→ new avalanches → permanent discharges !

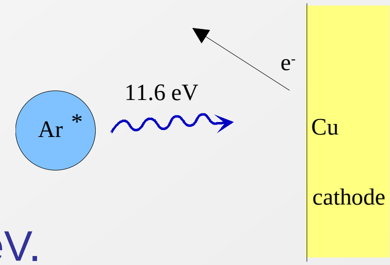

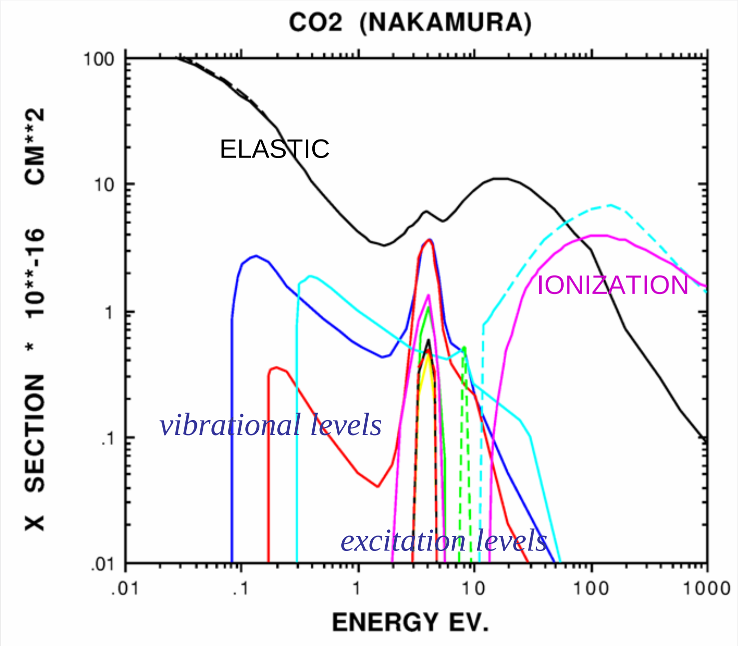

Solution: addition of polyatomic gas as a quencher

Absorption of photons in a large energy range (many vibrational and rotational energy levels).

Energy dissipation by collisions with gas molecules or dissociation into smaller molecules.

SWPC – Operation Modes

- ionization mode – full charge collection, but no charge multiplication;
  gain ~ 1
- proportional mode – multiplication of ionization starts; detected signal proportional to original ionization → possible energy measurement (dE/dx); secondary avalanches have to be quenched;
  gain ~ $10^4 – 10^5$
- limited proportional mode (saturated, streamer) – strong photoemission; secondary avalanches merging with original avalanche; requires strong quenchers or pulsed HV; large signals → simple electronics;
  gain ~ 10^{10}
- Geiger mode – massive photoemission; full length of the anode wire affected; discharge stopped by HV cut; strong quenchers needed as well

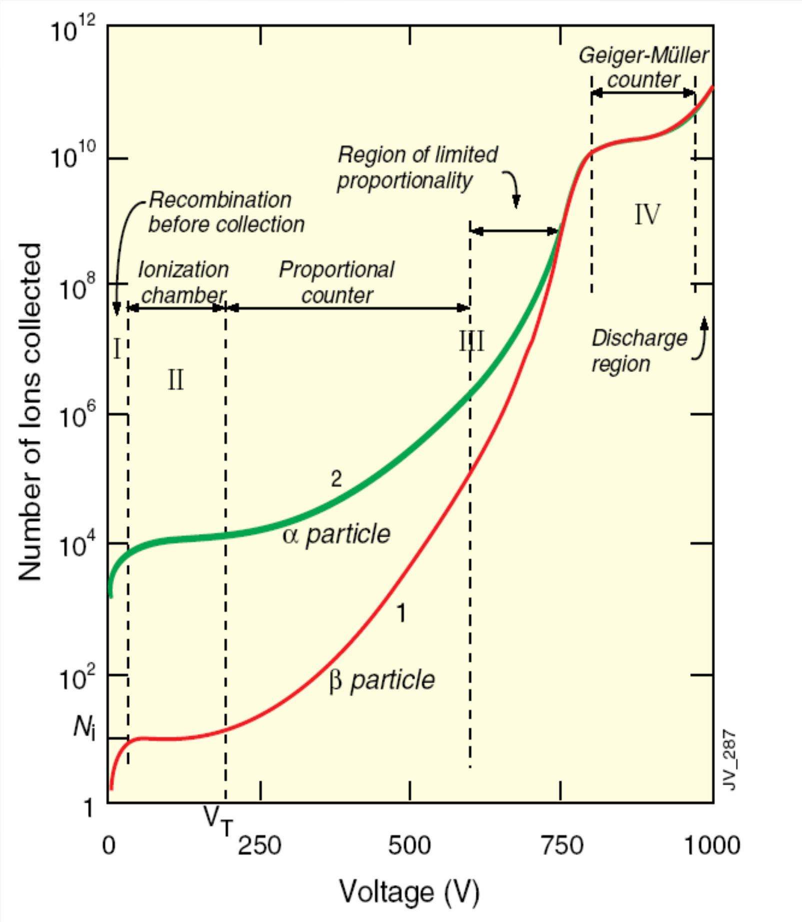

SWPC – Signal Formation

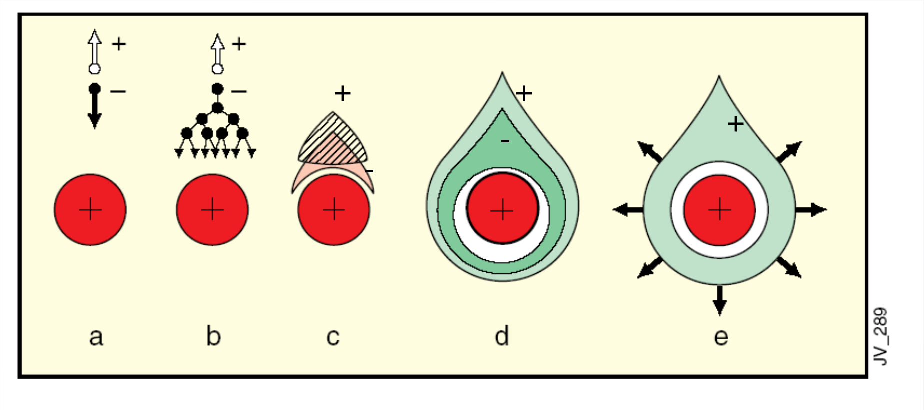

Avalanche formation within a few wire radii and within t < 1 ns.

Signal induction both on anode and cathode due to moving charges (both electrons and ions).

$$dv = \frac{Q}{lCV_0}\frac{dV}{dr}dr$$

Electrons collected by the anode wire i.e. dr is very small (few μm). Electrons contribute only very little to detected signal (few %).

Ions have to drift back to cathode i.e. dr is large (few mm). Signal duration limited by total ion drift time.

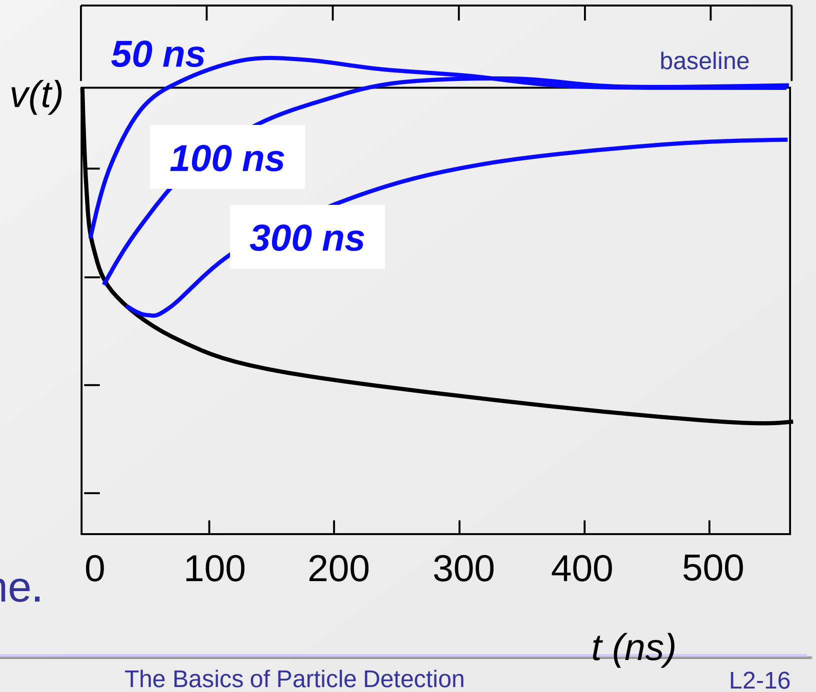

Need electronic signal differentiation to limit dead time.

Multiwire Proportional Chamber

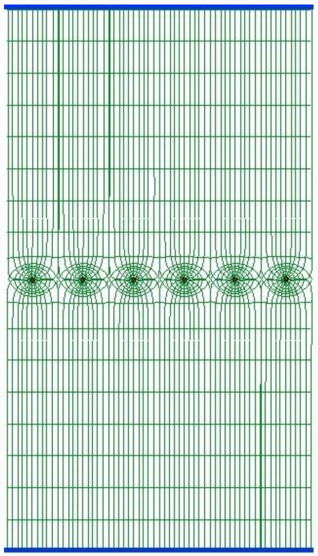

Simple idea to multiply SWPC cell : Nobel Prize 1992

First electronic device allowing high statistics experiments !!

Typical geometry

5mm, 1mm, 20 μm

Normally digital readout :

spatial resolution limited to

$$\sigma_x \approx \frac{d}{\sqrt{12}}$$

for d = 1 mm σ_x = 300 μm

G. Charpak, F. Sauli and J.C. Santiard

Cylindrical geometry is not the only one able to generate strong electric field:

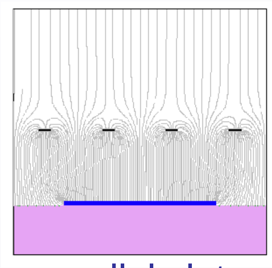
parallel plate

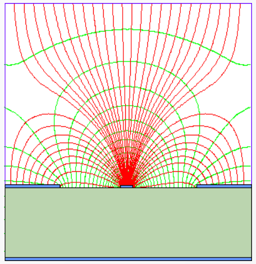
strip

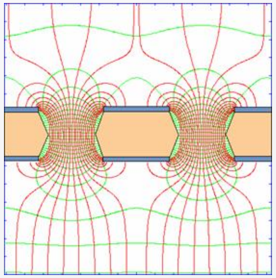
hole

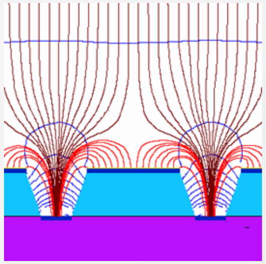
groove

MicroMegas

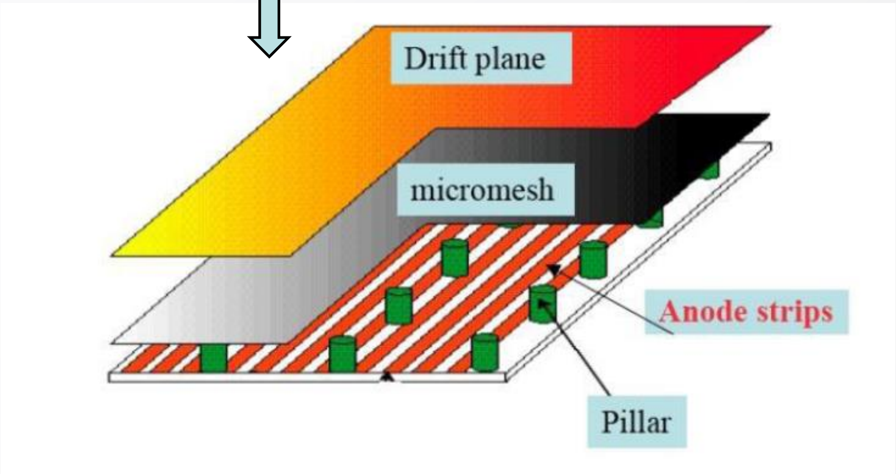

GEM

Ø 50-70 µm

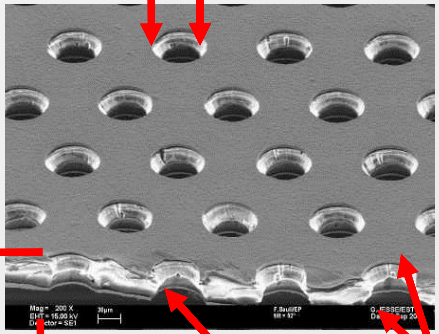

Kapton
Copper
HV

From 1D to 2D detectors

a)

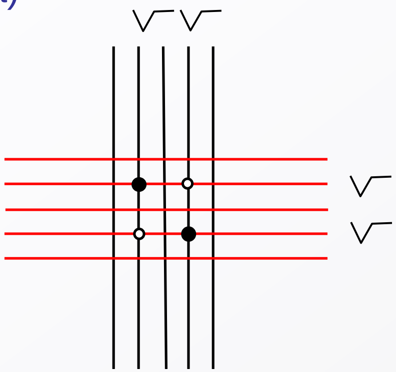

Crossed wire plane
→ 2N channels
However: ghost hits (≥2 particles)

b)

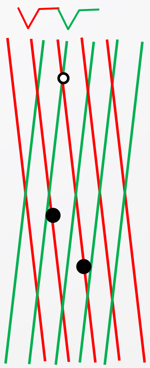

Stereo geometry (e.g. ±5°)
→ 2N channels.
One coordinate has worse resolution than other.
Ghost hits only local.

c)

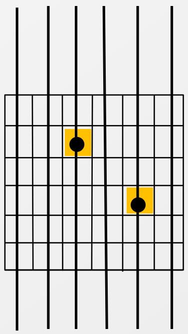

True 2D readout. Signals from wires are induced on readout plane just behind wires.
→ N^2 channels!

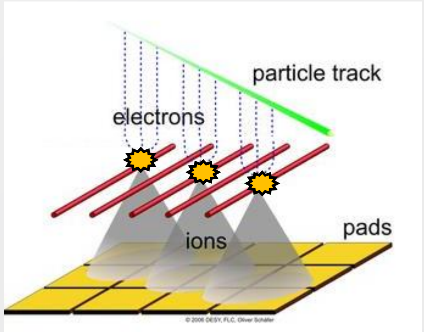

Drift Chambers

Spatial information obtained by measuring time of drift of electrons

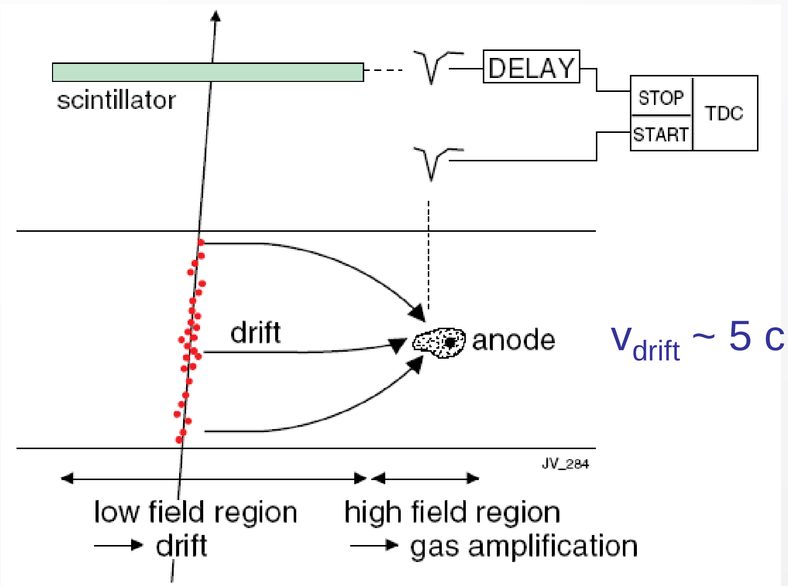

$v_{drift} \sim 5$ cm/μs

- Measure arrival time of electrons at sense wire relative to a time t_0.
- Need a trigger (bunch crossing or scintillator).
- Drift velocity independent from E.

F. Sauli, NIM 156(1978)147

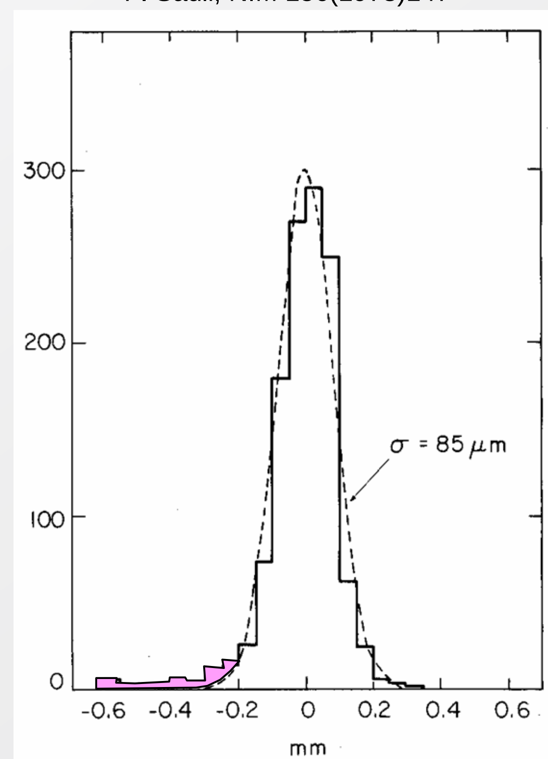

Advantages: smaller number of wires
→ less electronics channels.

Resolution determined by diffusion, primary ionization statistics, path fluctuations and electronics.

TPC – Time Projection Chamber

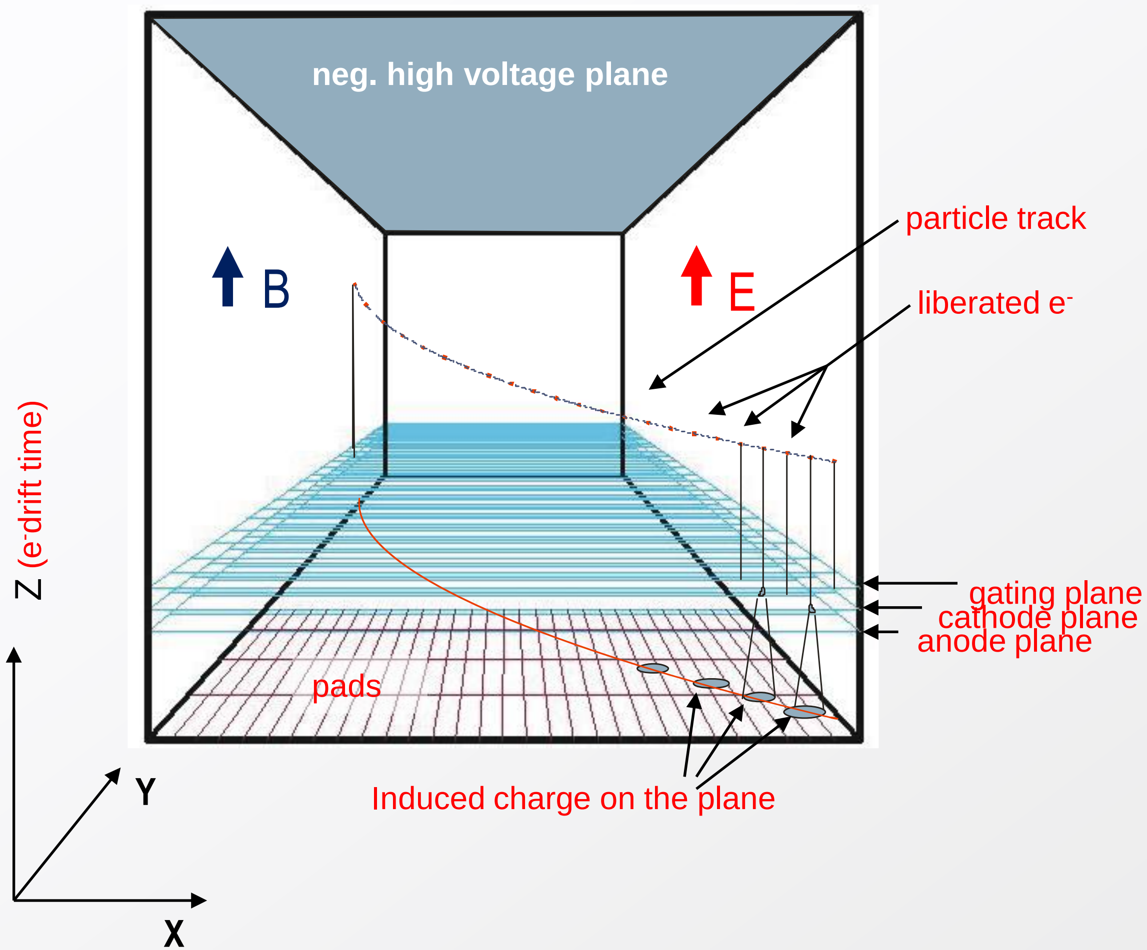

Time Projection Chamber

full 3D track reconstruction:

- x-y from wires and segmented cathode of MWPC (or GEM)
- z from drift time
- momentum measurement: space resolution + B field (multiple scattering)
- dE/dx measurement: measurement of primary ionization → ~ β
- Particle ID

$$m_0 = p/\beta\gamma c$$

TPC – Time Projection Chamber

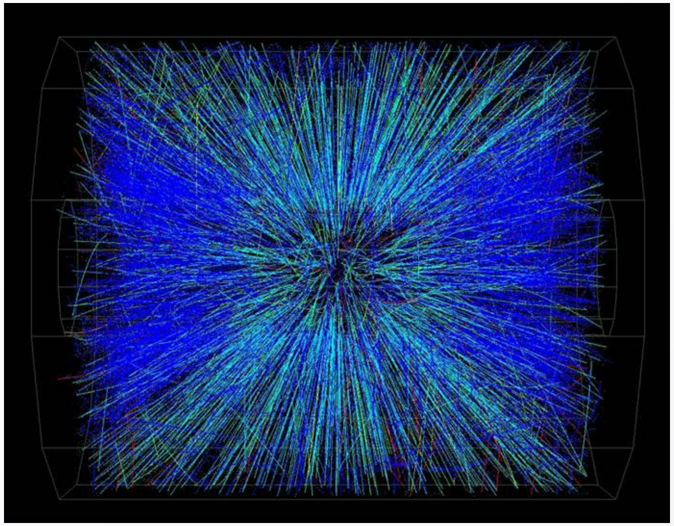

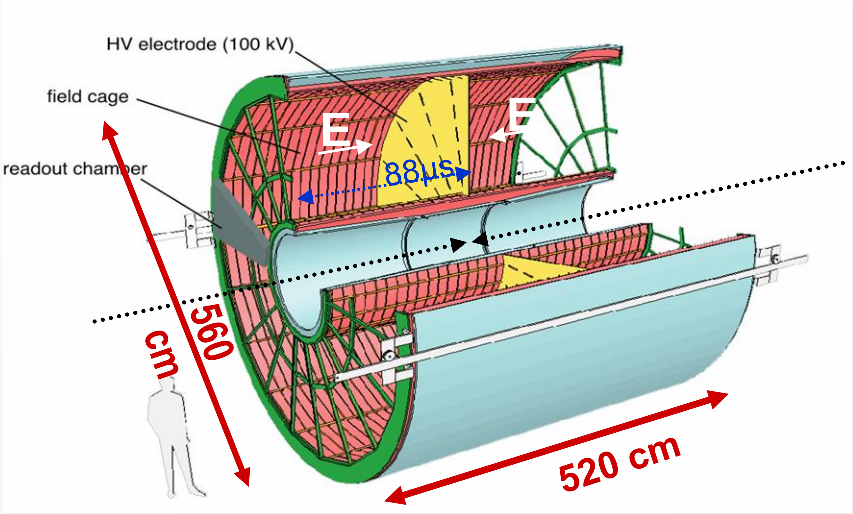

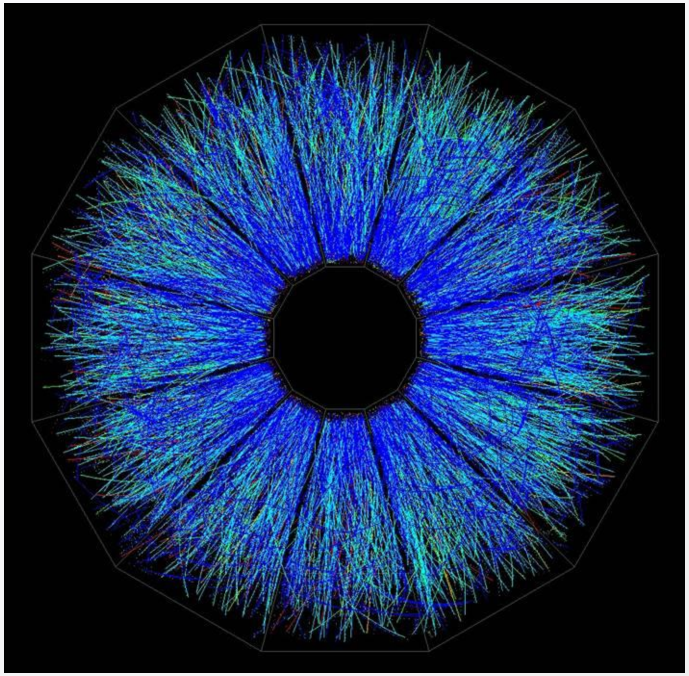

Alice TPC

HV central electrode at –100 kV

Drift length 250 cm at E = 400 V/cm

Gas Ne-CO_2 90-10

Space point resolution ~500 μm

dp/p = 2%@1GeV/c; 10%@10 GeV/c

Events from STAR TPC at RHIC

Au-Au collisions at CM energy of 130 GeV/n

Typically ~2000 tracks/event

Gas Detectors in LHC Experiments

ALICE: TPC (tracker), TRD (transition rad.), TOF (MRPC), HMPID (RICH-pad chamber), Muon tracking (pad chamber), Muon trigger (RPC)

ATLAS: TRD (straw tubes), MDT (muon drift tubes), Muon trigger (RPC, thin gap chambers)

CMS: Muon detector (drift tubes, CSC), RPC (muon trigger)

LHCb: Tracker (straw tubes), Muon detector (MWPC, GEM)

TOTEM: Tracker & trigger (CSC , GEM)

Solid state detectors = mostly Silicon detectors

We are looking for a detector to overcome some of the limitations of the gaseous detectors

- Small primary signal → need of gas amplification (not discussed: aging, rate limitations)
- Moderate spatial resolution (100 um)
- Massive frames, high voltage, gas circulation

Silicon (also GaAs, diamond) is a very promising material

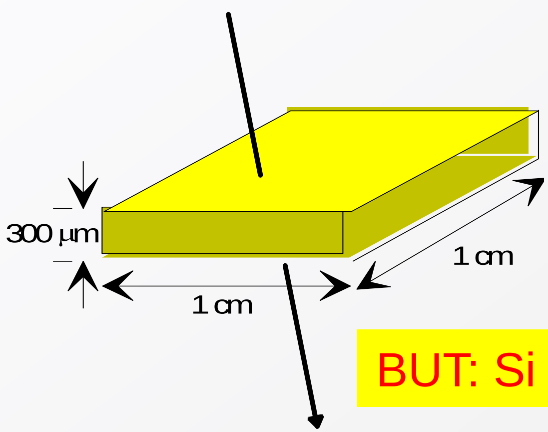

- ultra pure crystalline material
- $\rho_{Si} = 2.33$ g/cm^3
- Energy loss of particles in Si = 3.8 MeV/cm
- E(e-h pair) = 3.6 eV (≈ 20-30 eV for gas detectors)
- A particle traversing 300 μm of Si creates **~30'000** e/h pairs

BUT: Si is a semiconductor. It contains already free charge carriers.

At room temperature, in 1 x 1 x 0.03 cm^3, there are **$4.5 \cdot 10^8$** free charge carriers. We have to eliminate the free charges (= deplete the detector), such that our signal can be seen.

→ Use the principle of the pn junction

1. Dope Silicon with acceptor and donor atoms

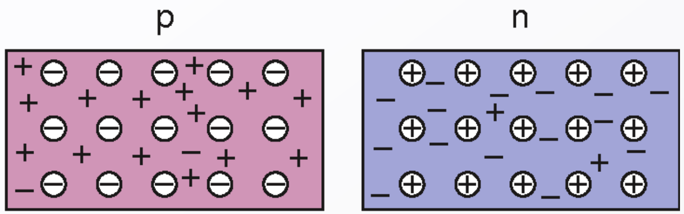

Boron: extra free holes
→ p-Si

Phosphor: extra free electrons
→ n-Si

2. Bring the two doped regions in contact

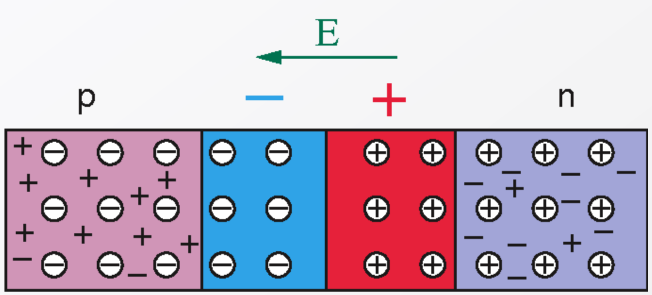

3. In the interface region holes and electrons will neutralise each other and create a depleted zone without any free charge carriers.

4. The resulting electric field separates newly created free charges → signal current

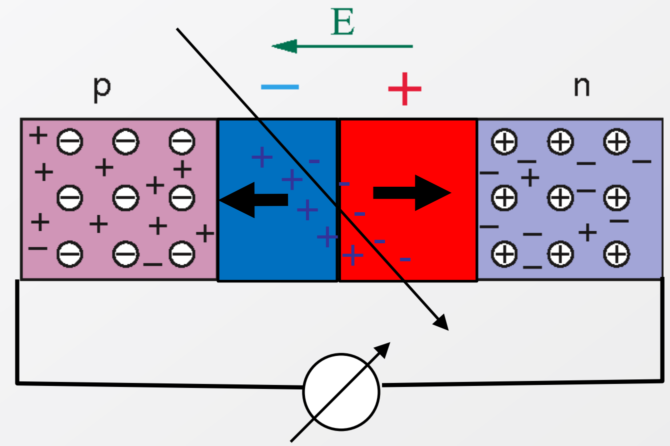

5. An external (reverse bias) voltage depletes the whole volume and makes it sensitive.

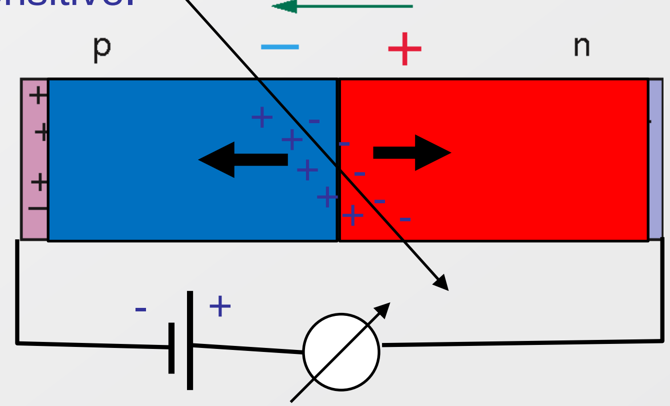

In the real world, Si-sensors are not produced by joining p and n doped material, but by implanting acceptors in a n-doped bulk (or donors in a p-doped bulk)

Simplest example: **(PIN) photodiode**

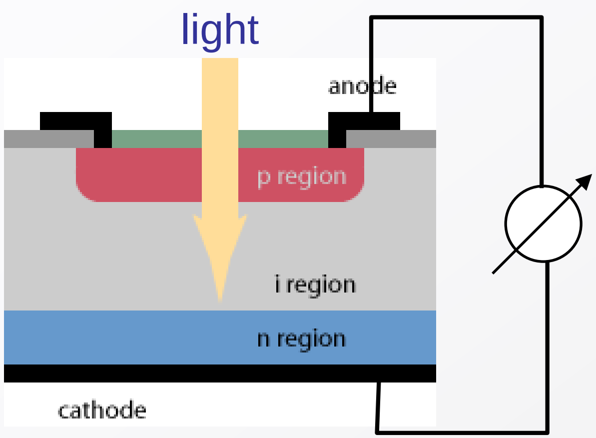

More complex: **Si microstrip detector**

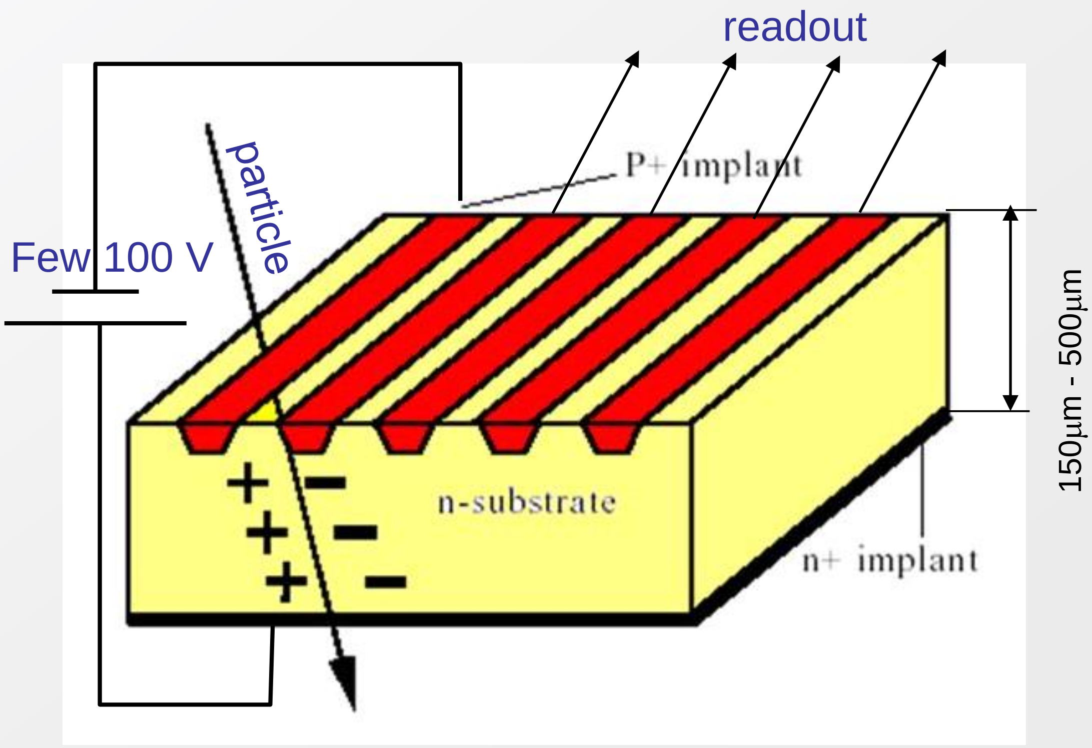

Si microstrip detector

Highly segmented silicon detectors have been used in Particle Physics experiments for 30 years.

They are favourite choice for Tracker and Vertex detectors (high resolution, speed, low mass, relatively low cost)

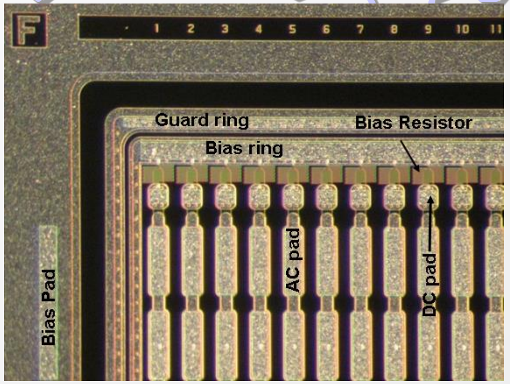

A real detector with 2 sensors, pitch adaptor, readout electronics and flex cable

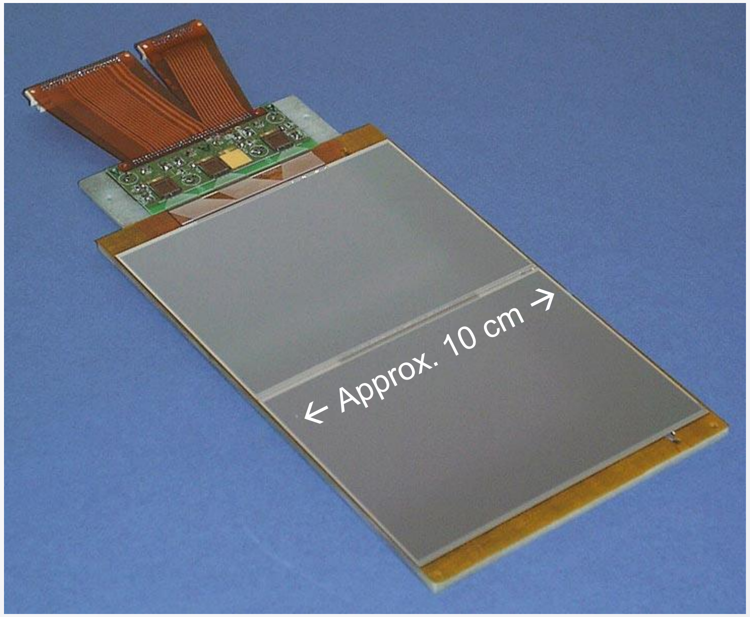

Pitch ~ 50µm

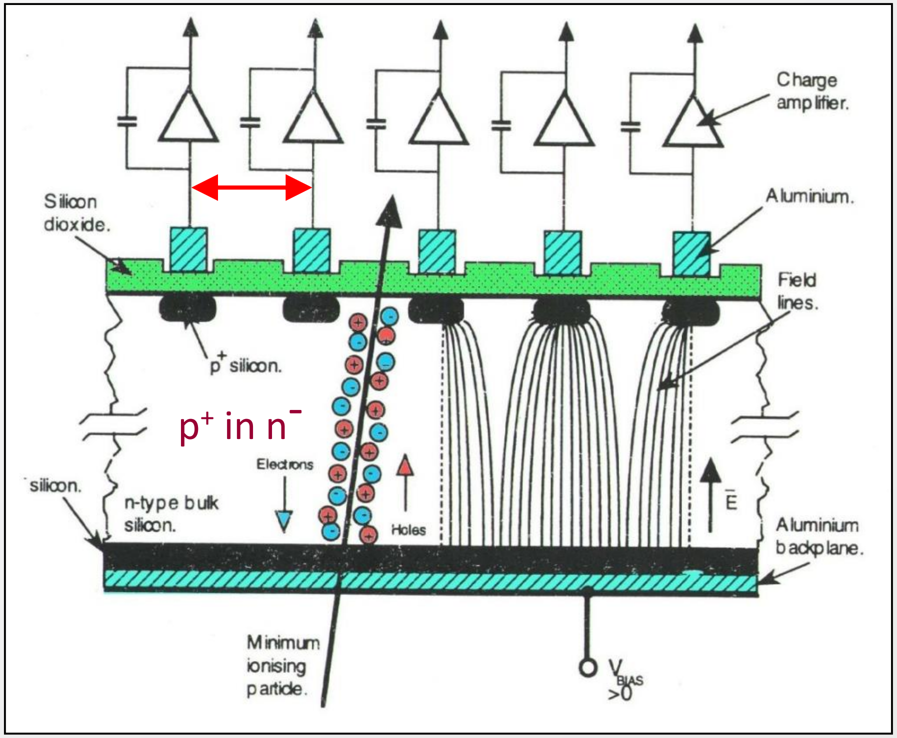

Resolution ~ 5µm

Si pixel detector

- HAPS – Hybrid Active Pixel Sensor
- segment silicon to diode matrix with high granularity readout (⇒ true 2D, no reconstruction ambiguity)
- electronic with same geometry (every cell connected to its own processing electronics)
- connection by "bump bonding"
- requires sophisticated readout architecture
- Hybrid pixel detectors are/will be used in LHC experiments: ATLAS, ALICE, CMS and LHCb

Solder Bump: Pb-Sn

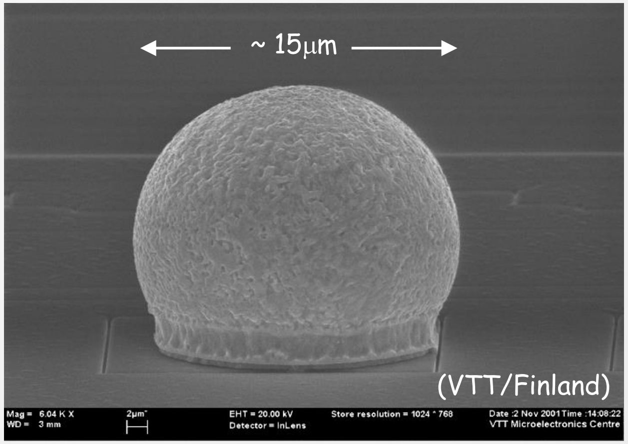

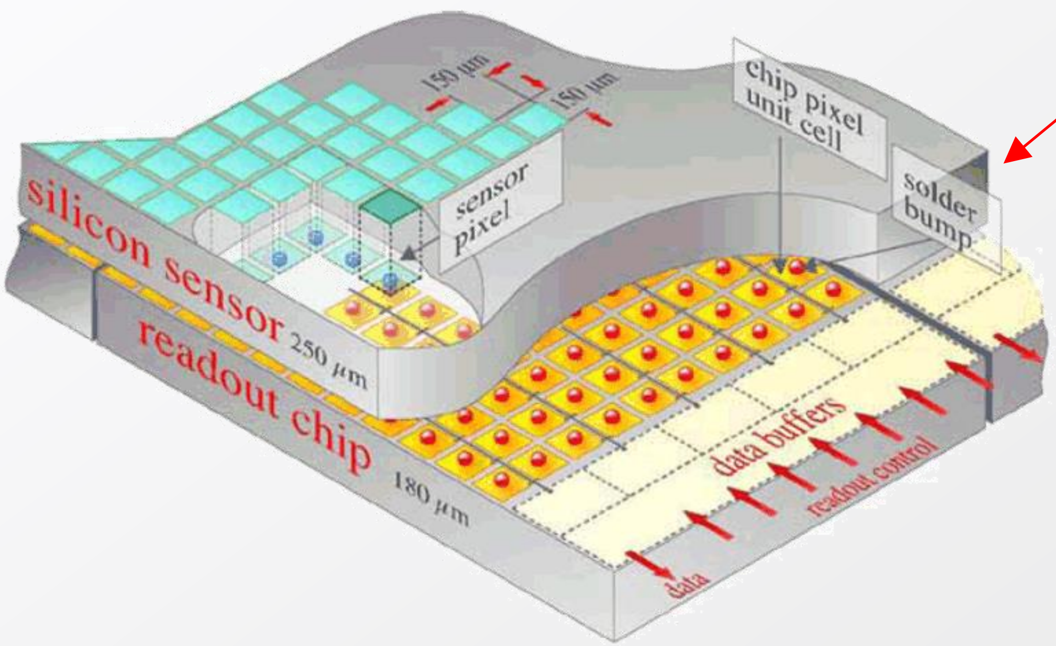

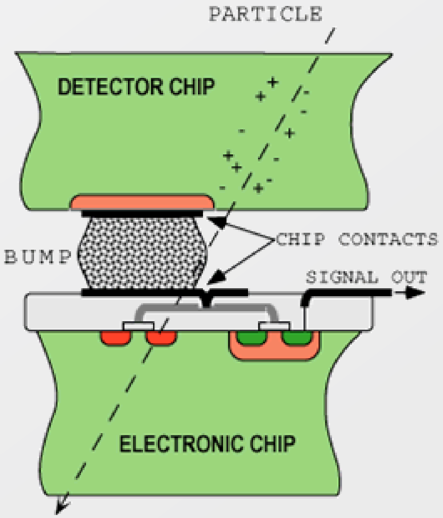

Flip-chip technique

Particle Identification via their lifetime

High resolution silicon detectors allow to observe secondary and tertiary vertices.

PV	SV	TV
$pp \rightarrow x + \bar{B}_s$	$\bar{B}_s \rightarrow D_s^+ + \mu^-$	$D_s^+ \rightarrow \pi + K^+ + K^-$

$\tau_0(B_s) \approx 1.5$ ps

$\tau_0(D_s^+) \approx 0.4$ ps

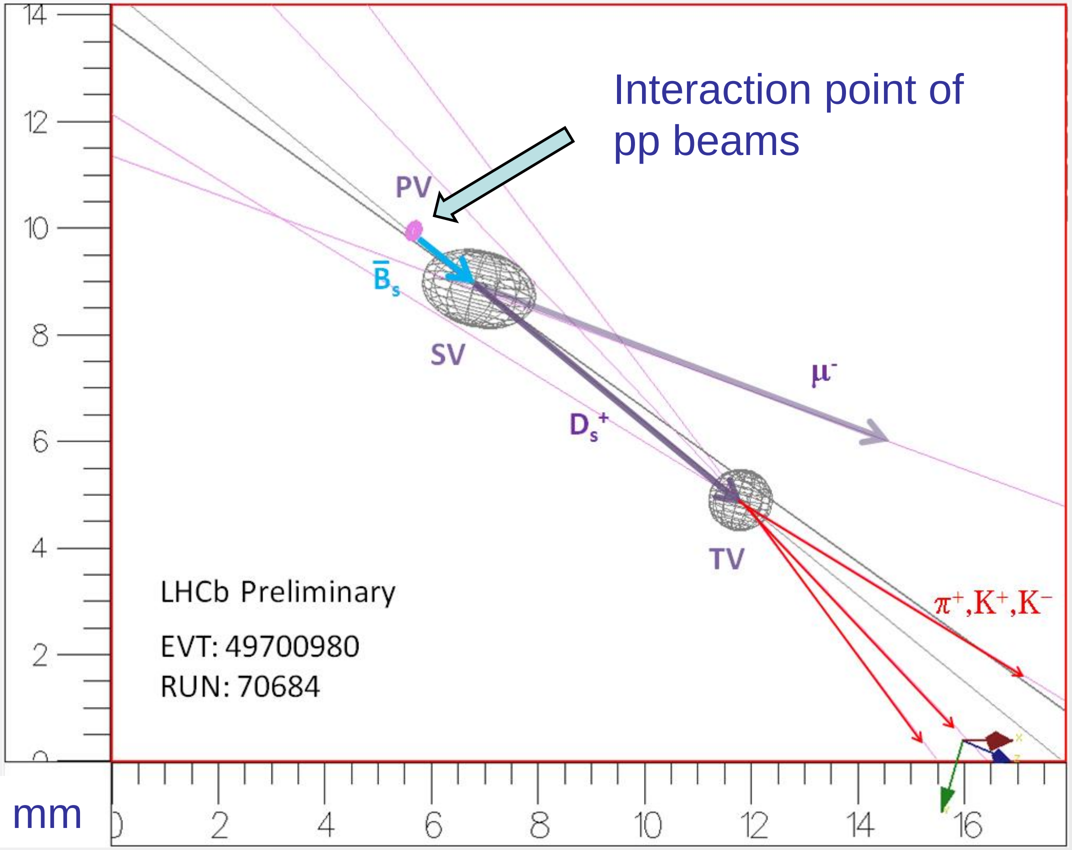

scale in mm

Silicon tracking detectors are used in all LHC experiments:
Different sensor technologies, designs, operating conditions,….

ALICE Pixel Detector

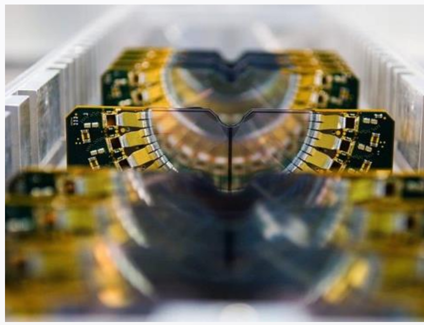

LHCb VELO

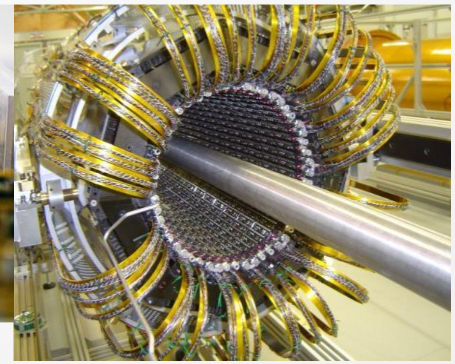

ATLAS Pixel Detector

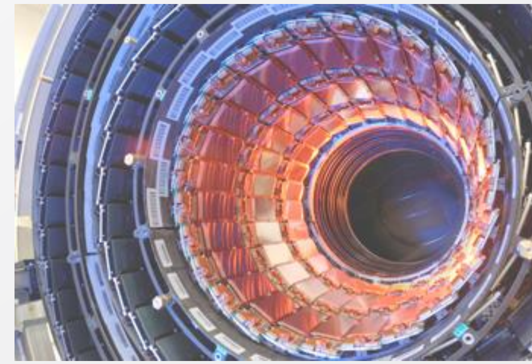

CMS Strip Tracker IB

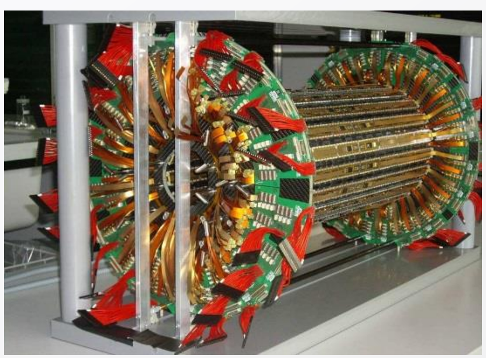

CMS Pixel Detector

ALICE Drift Detector

ALICE Strip Detector

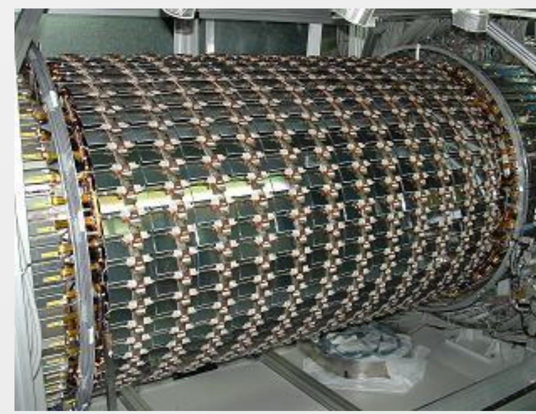

ATLAS SCT Barrel

P.Riedler, ECFA Workshop, Oct.2013

Interaction of charged particles

Energy loss by Bremsstrahlung

Radiation of real photons in the Coulomb field of the nuclei of the absorber medium

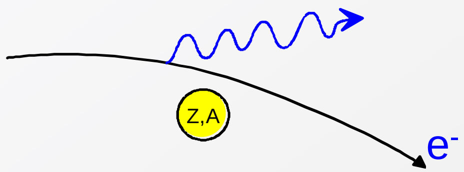

$$-\frac{dE}{dx} = 4\alpha N_A \frac{Z^2}{A} z^2 \left(\frac{1}{4\pi\varepsilon_0}\frac{e^2}{mc^2}\right)^2 E \ln\frac{183}{Z^{1/3}} \propto \frac{E}{m^2}$$

Effect is only relevant for e± and ultra-relativistic μ (>1000 GeV)

$$\frac{m_\mu^2}{m_e^2} = \frac{105^2\,\mathrm{MeV}^2}{0.5^2\,\mathrm{MeV}^2} = 4.4\cdot 10^4$$

For electrons:

$$-\frac{dE}{dx} = 4\alpha N_A \frac{Z^2}{A} r_e{}^2 E \ln\frac{183}{Z^{1/3}}$$

$$-\frac{dE}{dx} = \frac{E}{X_0}$$

energy loss is proportional to actual energy

$$\Rightarrow \quad E = E_0\, e^{-x/X_0}$$

$$X_0 = \frac{A}{4\alpha N_A Z^2 r_e{}^2 \ln\frac{183}{Z^{1/3}}}$$

radiation length [g/cm²]

(divide by specific density to get X_0 in cm)

Interaction of charged particles

Critical energy E_c

$$\frac{dE}{dx}(E_c)\Big|_{Brems} = \frac{dE}{dx}(E_c)\Big|_{ion}$$

For electrons one finds approximately:

$$E_c^{solid+liq} = \frac{610\,\mathrm{MeV}}{Z+1.24} \qquad E_c^{gas} = \frac{710\,\mathrm{MeV}}{Z+1.24}$$

$E_c(e^-)$ in Cu ($Z=29$) = 20 MeV

For muons $E_c \approx E_c^{elec}\left(\frac{m_\mu}{m_e}\right)^2$

$E_c(\mu)$ in Cu $\approx$ 1 TeV

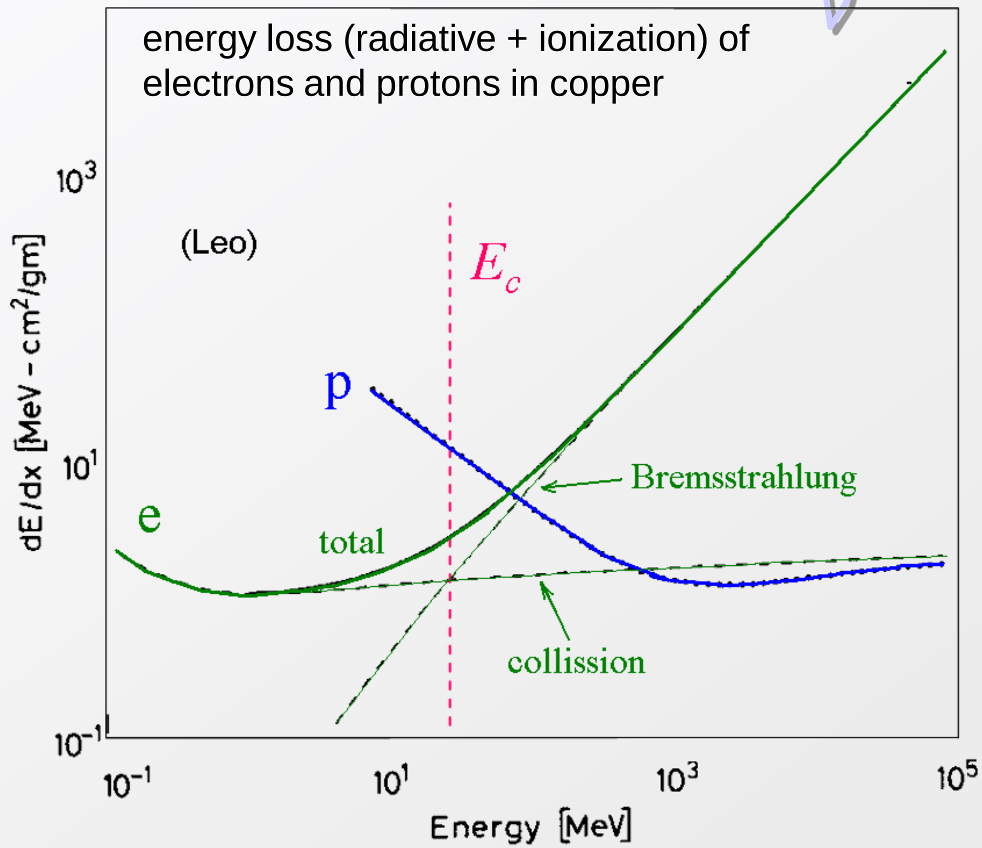

Unlike electrons, muons in multi-GeV range can traverse thick layers of dense matter.
Find charged particles traversing the calorimeter ? → most likely a muon → Particle ID

Interaction of photons

In order to be detected, a photon has to create charged particles and / or transfer energy to charged particles

Photo-electric effect:

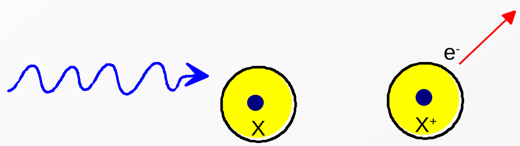

$$\gamma + \text{atom} \rightarrow \text{atom}^{+} + e^{-}$$

Only possible in the close neighborhood of a third collision partner → photo effect releases mainly electrons from the K-shell.

Cross section shows strong modulation if $E_\gamma \approx E_{shell}$

$$\sigma^{K}_{photo} = \left(\frac{32}{\varepsilon^7}\right)^{\frac{1}{2}} \alpha^4 Z^5 \sigma^{e}_{Th} \qquad \varepsilon = \frac{E_\gamma}{m_e c^2} \qquad \sigma^{e}_{Th} = \tfrac{8}{3}\pi r_e^2 \quad \text{(Thomson)}$$

At high energies ($\varepsilon \gg 1$)

$$\sigma^{K}_{photo} = 4\pi r_e^2 \alpha^4 Z^5 \frac{1}{\varepsilon} \qquad \boxed{\sigma_{photo} \propto Z^5}$$

Interaction of photons

Compton scattering:

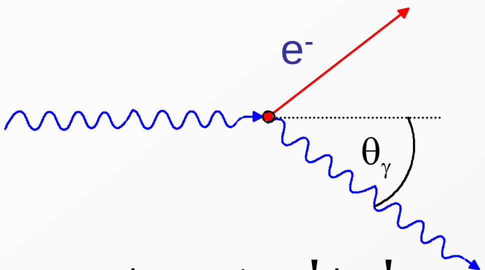

$$\gamma + e \rightarrow \gamma' + e'$$

$$E'_\gamma = E_\gamma \frac{1}{1+\varepsilon(1-\cos\theta_\gamma)} \qquad \varepsilon = \frac{E_\gamma}{m_e c^2}$$

$$E_e = E_\gamma - E'_\gamma$$

Compton cross-section (Klein-Nishina)
example: E_γ = 0 … 511 keV

Assume electron as quasi-free.

Klein-Nishina $\frac{d\sigma}{d\Omega}(\theta,\varepsilon)$ →

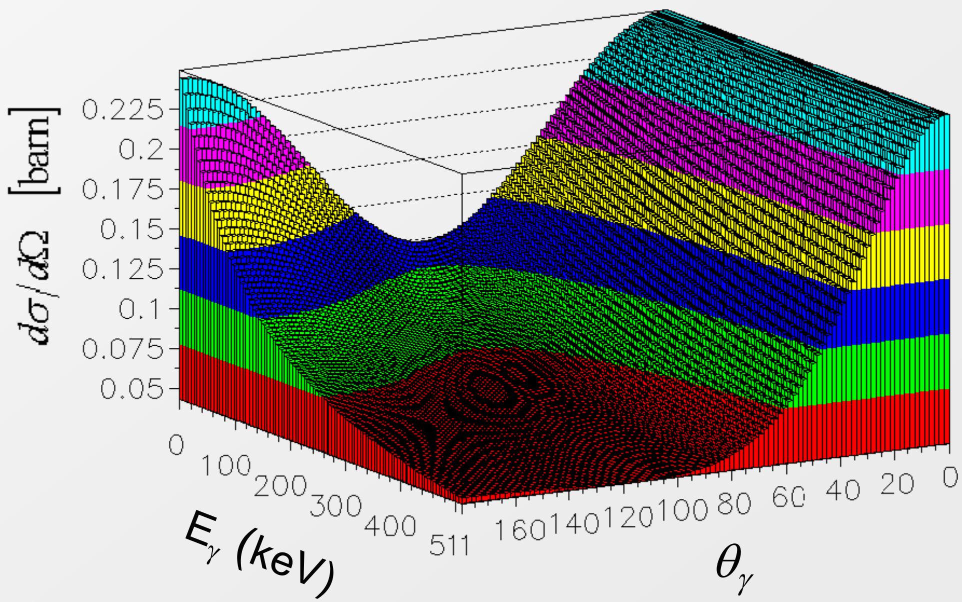

At high energies approximately

$$\sigma_c^e \propto \frac{\ln\varepsilon}{\varepsilon}$$

Atomic Compton cross-section:

$$\sigma_c^{atomic} = Z \cdot \sigma_c^e$$

Detection of 511 keV (annihilation) photons in a LYSO crystal scintillator

($Lu_{(2-x)}Y_xSiO_5$ (with x~0.1-0.2))

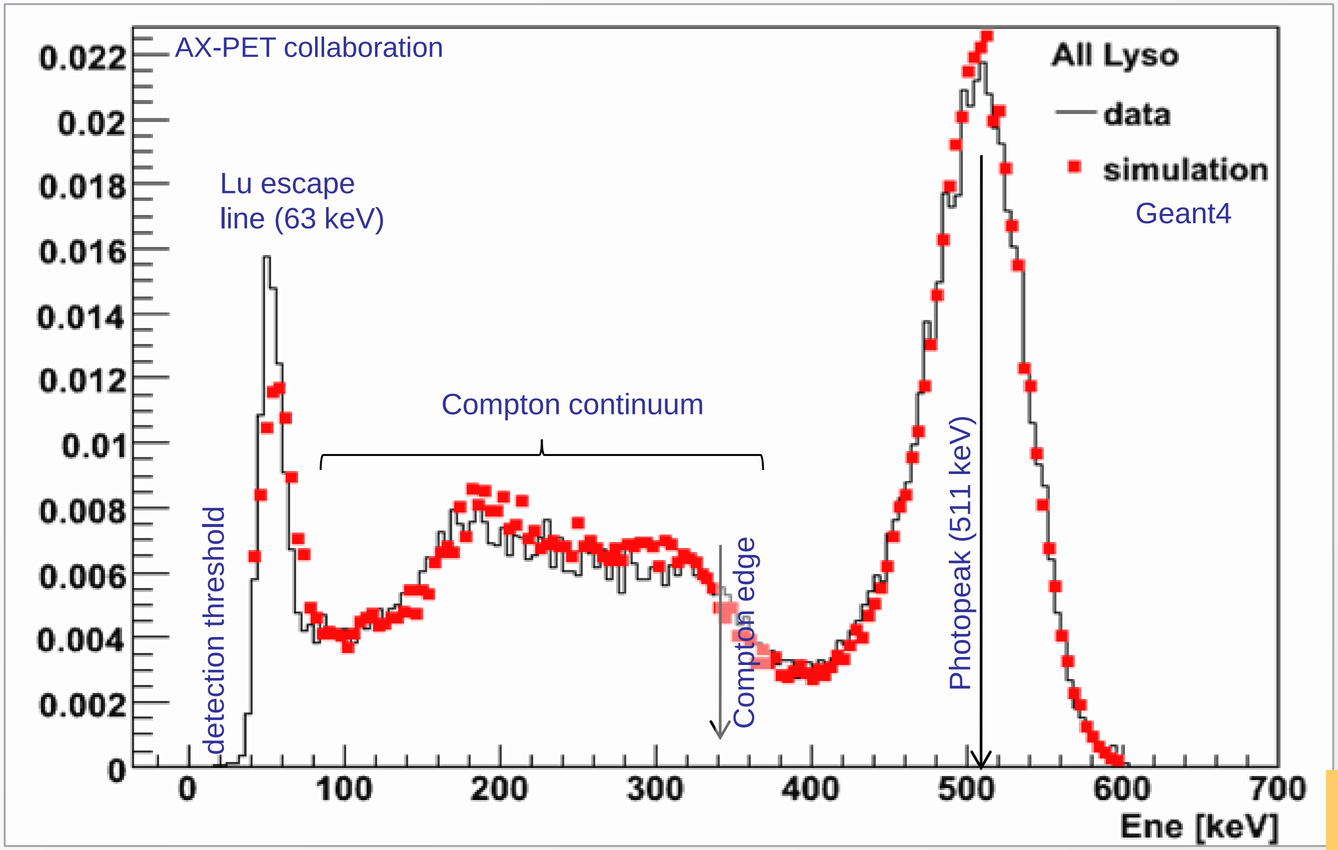

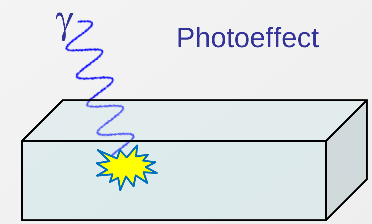

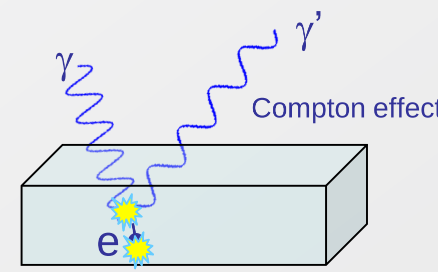

Relative stregths of photopeak and Compton continuum depend on Z_{eff} of scintillator and geometry.

Compton: $E'_\gamma = E_\gamma \dfrac{1}{1+\varepsilon(1-\cos\theta_\gamma)}$ $\quad \varepsilon = \dfrac{E_\gamma}{m_e c^2}$ $\quad E_\gamma = 511\,\text{keV} \rightarrow \varepsilon = 1$

$$E'^{\,\min}_\gamma = E'_\gamma(\theta = 180°) = E_\gamma \frac{1}{1+2\varepsilon} = E_\gamma / 3 \approx 170\,\text{keV} \qquad E_e^{\max} = E_\gamma - E'^{\,\min}_\gamma = 511 - 170 = 340\,\text{keV}$$

Interaction of photons

- **Pair production**

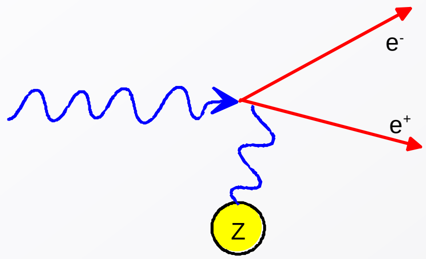

$$\gamma + nucleus \rightarrow e^+e^- + nucleus$$

Only possible in the Coulomb field of a nucleus (or an electron) if $E_\gamma \geq 2m_ec^2$

Cross-section (high energy approximation)

$$\sigma_{pair} \approx 4\alpha r_e^2 Z^2 \left(\frac{7}{9}\ln\frac{183}{Z^{\frac{1}{3}}}\right)$$

independent of energy !

$$\approx \frac{7}{9}\frac{A}{N_A}\frac{1}{X_0}$$

$$\approx \frac{A}{N_A}\frac{1}{\lambda_{pair}}$$

$$\lambda_{pair} = \frac{9}{7}X_0$$

Energy sharing between e^+ and e^- becomes asymmetric at high energies.

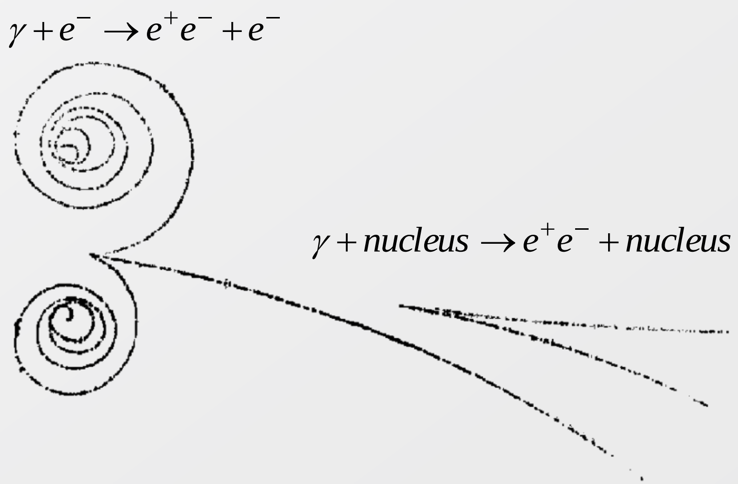

Interaction of photons

In summary: $I_\gamma = I_0 e^{-\mu x}$

μ: mass attenuation coefficient $\mu_i = \frac{N_A}{A}\sigma_i \quad \left[cm^2/g\right]$ $\quad \mu = \mu_{photo} + \mu_{Compton} + \mu_{pair} + \ldots$

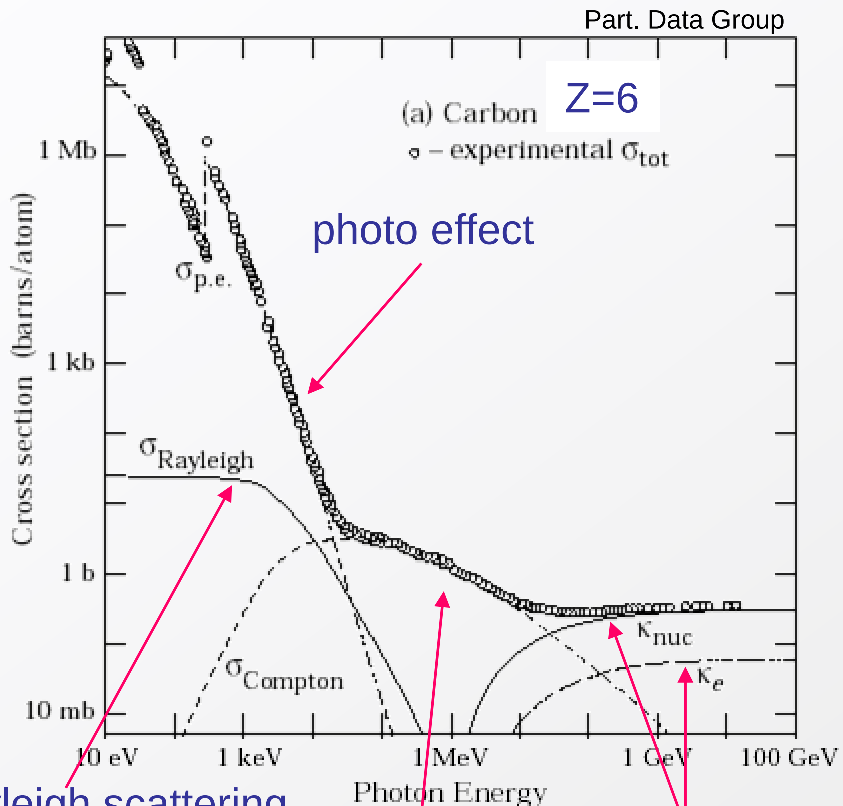

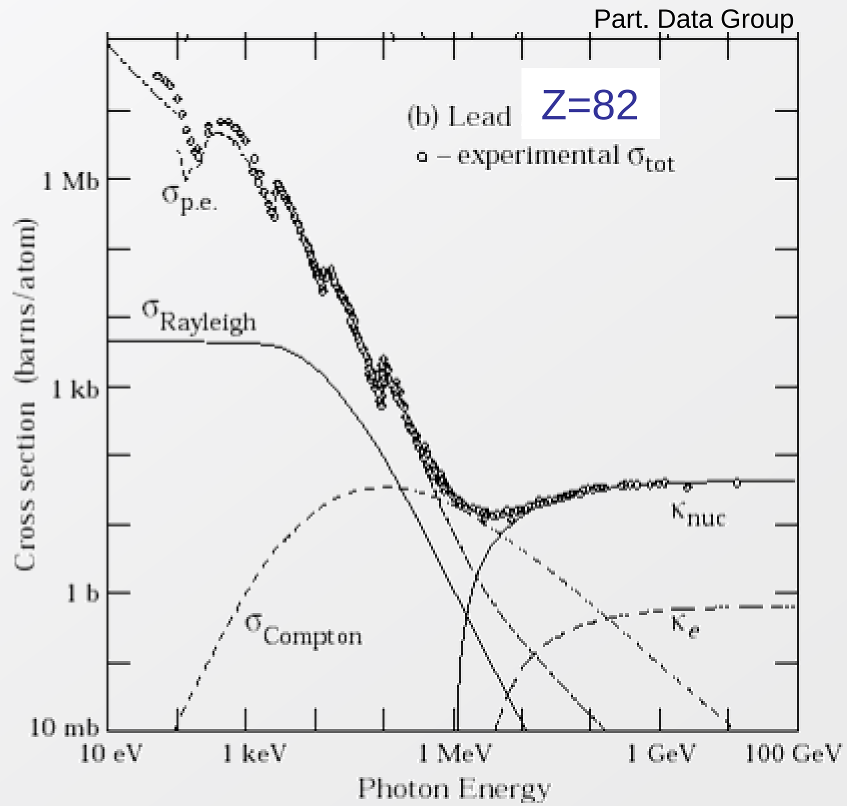

Rayleigh scattering
(no energy loss !)

pair production

Compton scattering

Summary: basic electromagnetic interactions

e^+ / e^-

- Ionisation

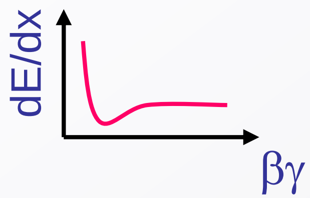

- Bremsstrahlung

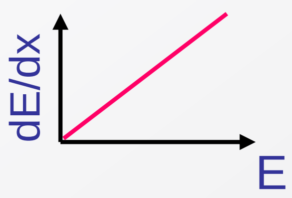

γ

- Photoelectric effect

- Compton effect

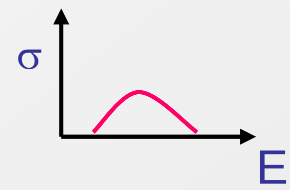

- Pair production

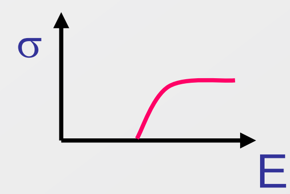

Backup slides

F. Sauli, IEEE Short Course on Radiation Detection and Measurement, Norfolk (Virginia) November 10-11, 2002

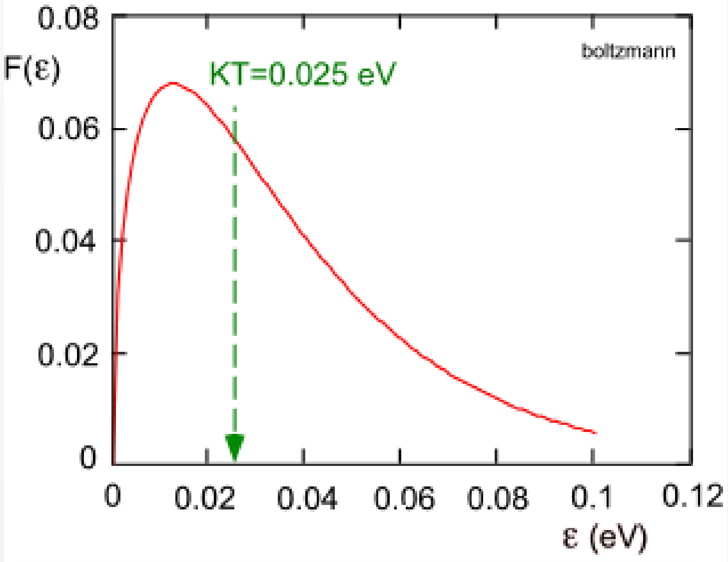

Free ionization charges lose energy in collisions with gas atoms and molecules (thermalization). They tend towards a Maxwell - Boltzmann energy distribution:

$$F(\varepsilon) \propto \sqrt{\varepsilon} \cdot e^{-\frac{\varepsilon}{kT}}$$

Average (thermal) energy:

$$\varepsilon_T = \frac{3}{2} kT \approx 0.040 eV$$

Diffusion equation:

Fraction of free charges at distance x after time t.

$$\frac{dN}{N} = \frac{1}{\sqrt{4\pi Dt}} e^{-\frac{x^2}{4Dt}} dt$$

D: diffusion coefficient

RMS of linear diffusion:

$$\sigma_x = \sqrt{2Dt}$$

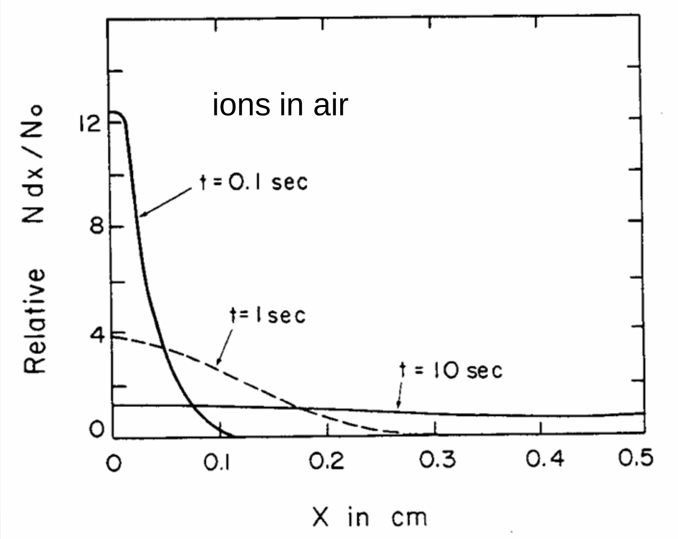

L.B. Loeb, Basic processes of gaseous electronics Univ. of California Press, Berkeley, 1961

Drift and Diffusion in Presence of E field

E=0 thermal diffusion $\langle v \rangle_t = 0$

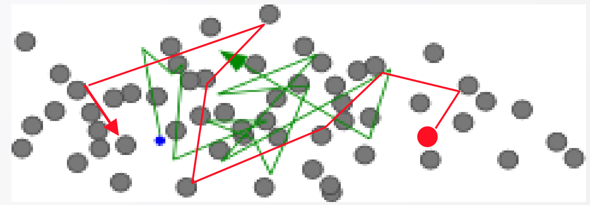

E>0 charge transport and diffusion $\langle v \rangle_t = v_D$

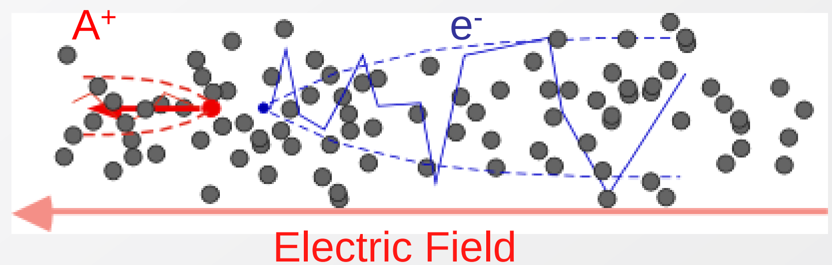

$$v_D = \frac{\Delta s}{\Delta t}$$ Drift velocity

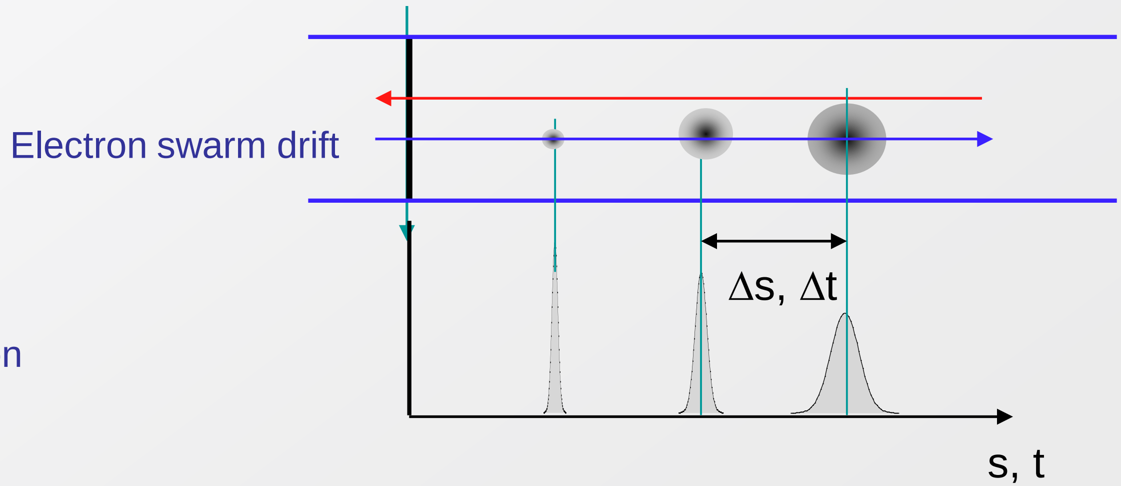

$$\sigma_x = \sqrt{2Dt} = \sqrt{2D\frac{s}{v_D}}$$ Diffusion

Townsend expression: $v_D = a\tau = \frac{eE}{m}\tau = \mu E$ (1)   τ = time between collisions $\tau = \frac{1}{N\sigma(\varepsilon)v}$ (2)

energy balance: $\frac{x}{v_D\tau}\lambda(\varepsilon)\varepsilon_E = eEx$ (3)   collision losses = energy gained in E-field

$\frac{x}{v_D\tau}$ number of collisions; $\lambda(\varepsilon)$ fractional energy loss per collision

ε_E equilibrium energy (excl. thermal motion) $\varepsilon_E = \frac{1}{2}mv^2$ (4) v instantaneous velocity

Insert (2) in (1) and then use (3) and (4) →

$$v_D^2 = \frac{eE}{mN\sigma(\varepsilon)}\sqrt{\frac{\lambda(\varepsilon)}{2}}$$

Drift is only possible if λ(ε) > 0 !

σ(ε) large → slow gas

σ(ε) small → fast gas

σ and λ are both functions of energy!

→ Parameters must be measured

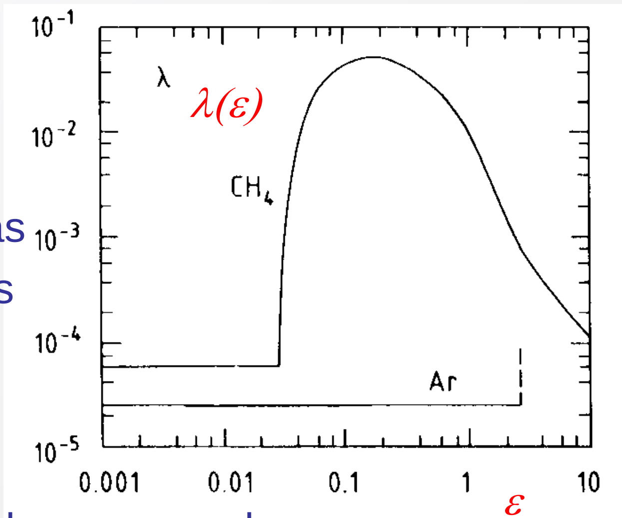

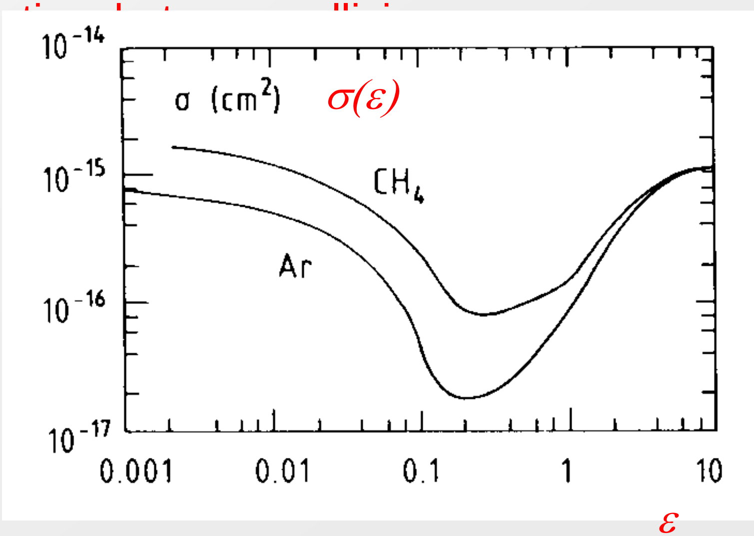

B. Schmidt, thesis, unpublished, 1986

CSC – Cathode Strip Chamber

Precise measurement of the second coordinate by interpolation of the signal induced on pads.

Closely spaced wires makes CSC fast detector.

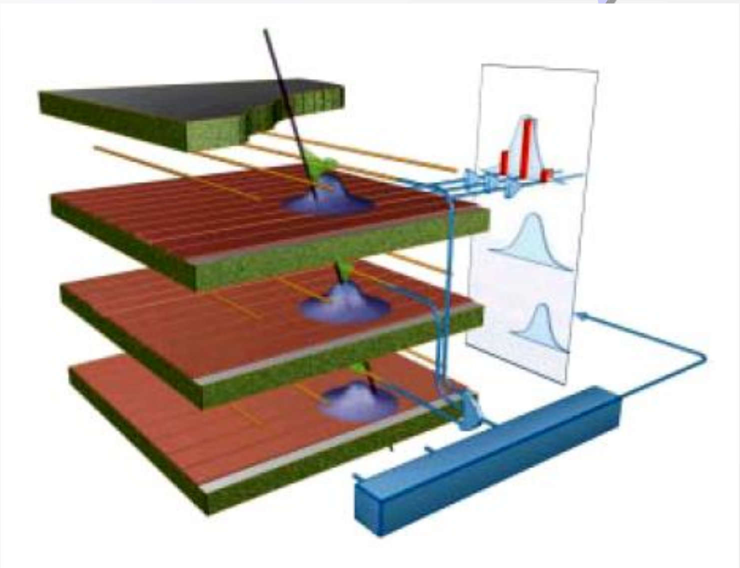

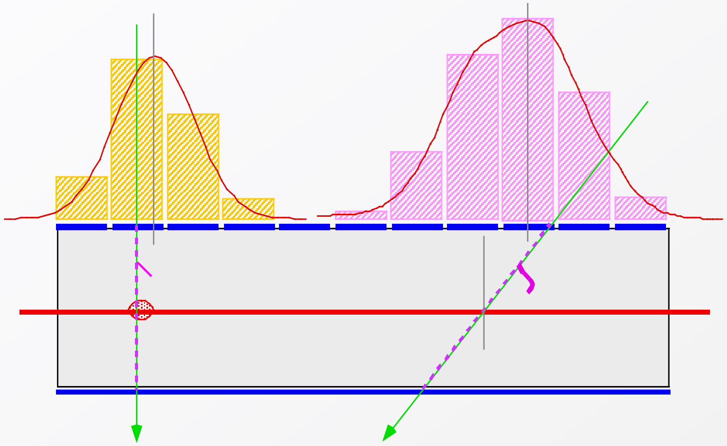

Center of gravity of induced signal method.

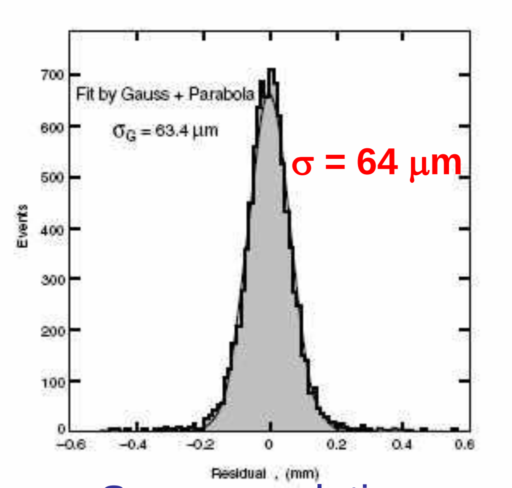

Space resolution

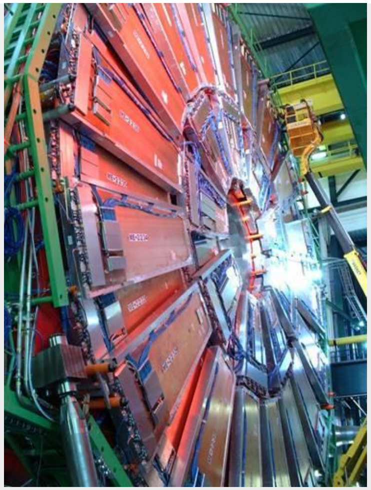

CMS

RPC – Resistive Plate Chamber

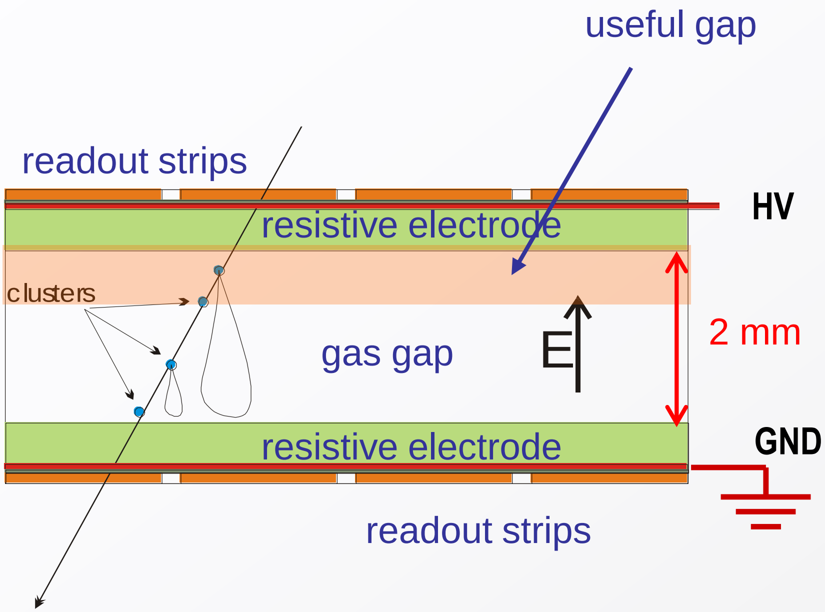

Operation at high E-field → streamer mode.
Rate capability strong function of the resistivity of electrodes.

MRPC

Multigap RPC - exceptional time resolution suited for TOF and trigger applications

A. Akindinov et al., NIM A456(2000)16

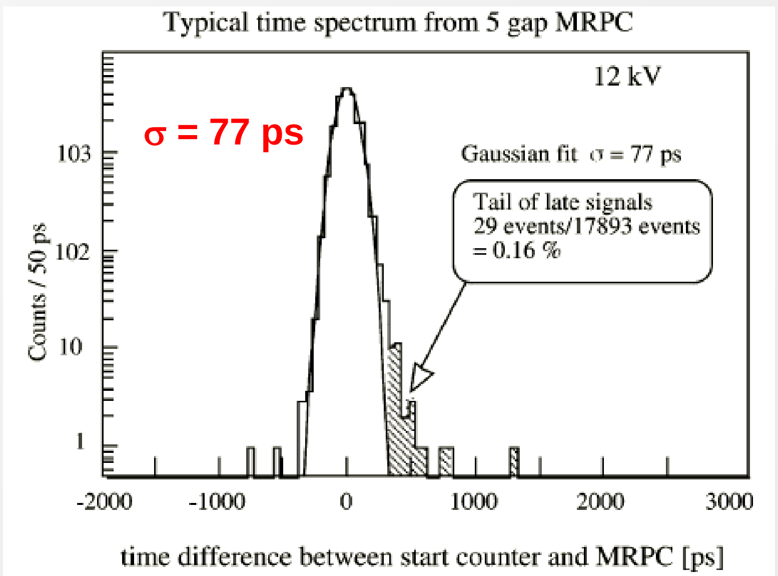

Time resolution

Large range of drift velocity and diffusion:

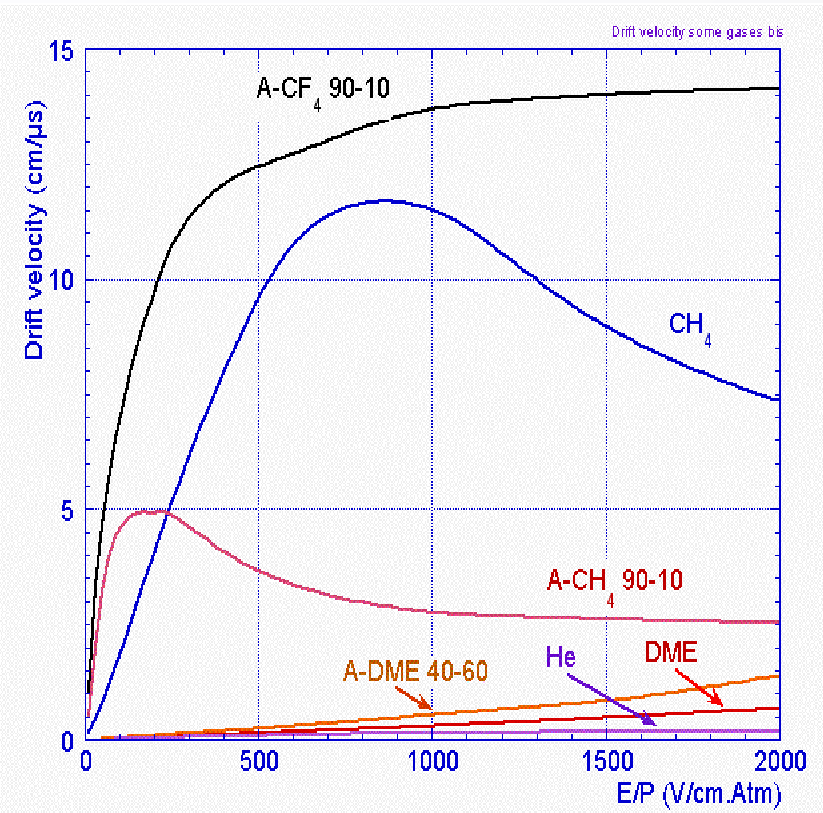

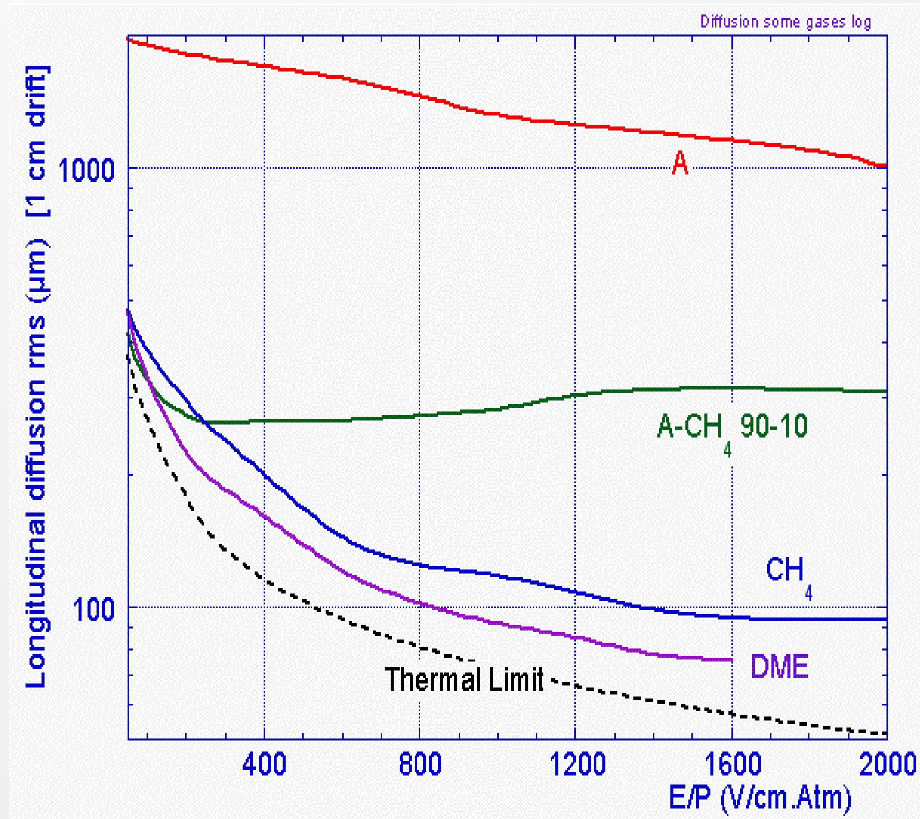

F. Sauli, IEEE Short Course on Radiation Detection and Measurement, Norfolk (Virginia) November 10-11, 2002

Rule of thumb: v_D (electrons) ~ 5 cm/μs = 50 μm / ns. Ions drift ~1000 times slower.

Diffusion Electric Anisotropy

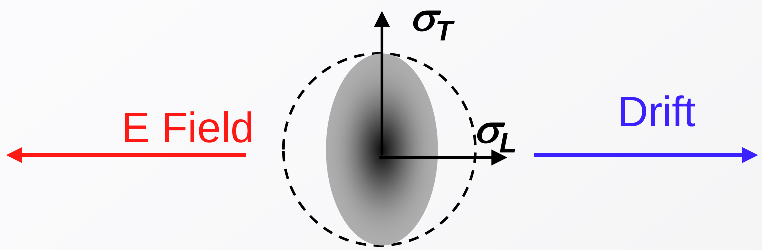

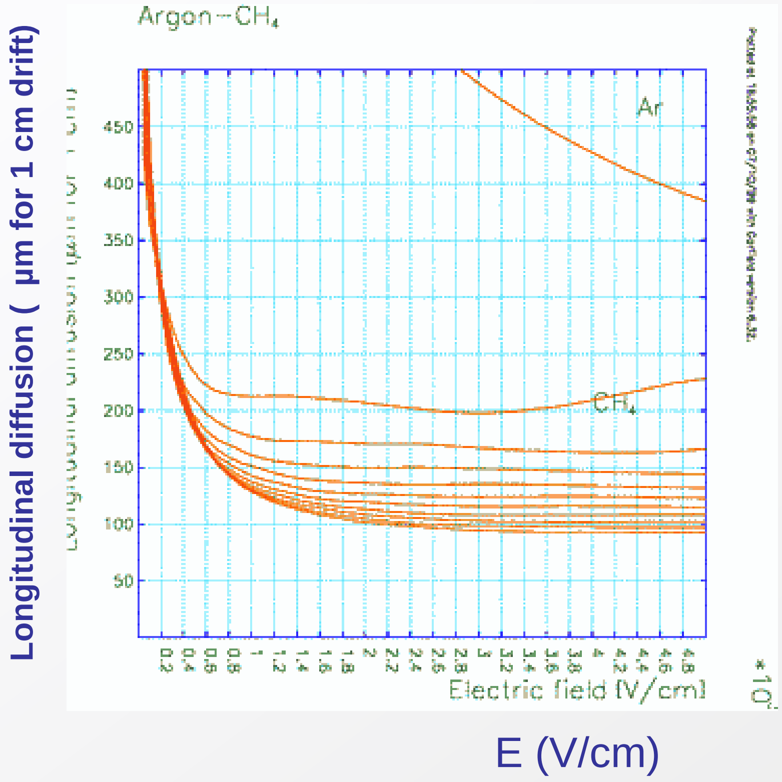

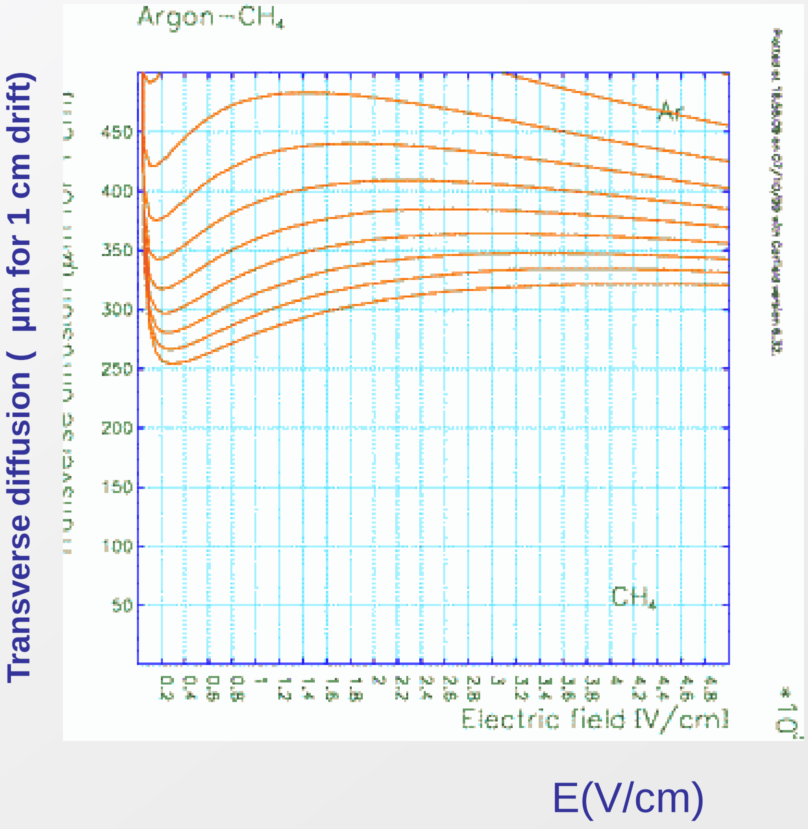

S. Biagi http://consult.cern.ch/writeup/magboltz/

Drift Chambers

Spatial information obtained by measuring time of drift of electrons

Measure arrival time of electrons at sense wire relative to a time t_0.

Need a trigger (bunch crossing or scintillator).

Drift velocity independent from E.

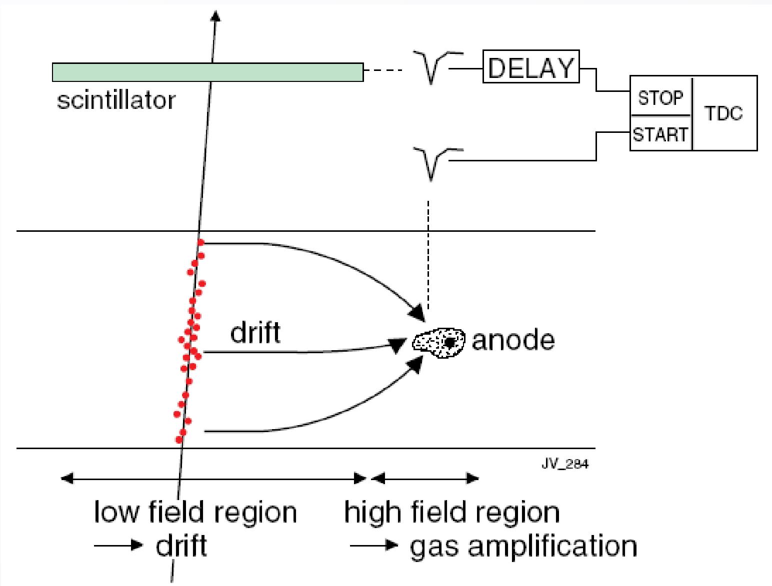

F. Sauli, NIM 156(1978)147

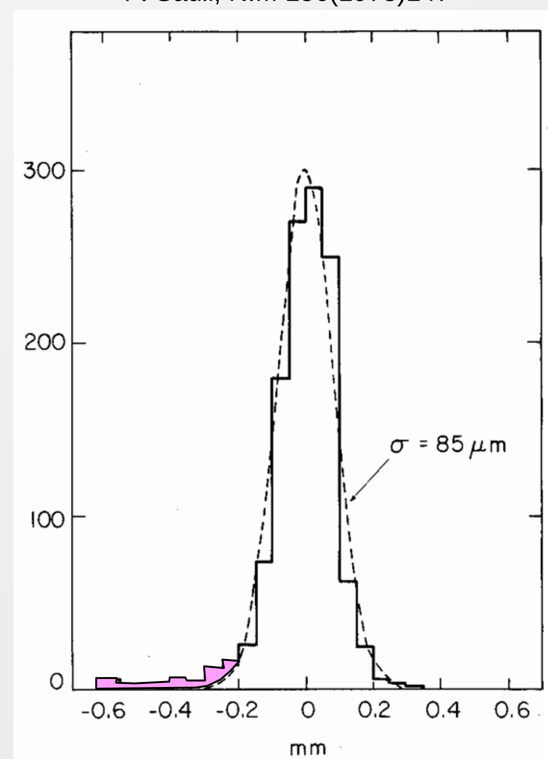

Advantages: smaller number of wires → less electronics channels.

Resolution determined by diffusion, primary ionization statistics, path fluctuations and electronics.

Planar drift chamber designs

Essential: linear space-time relation; constant E-field; little dpendence of v_D on E.

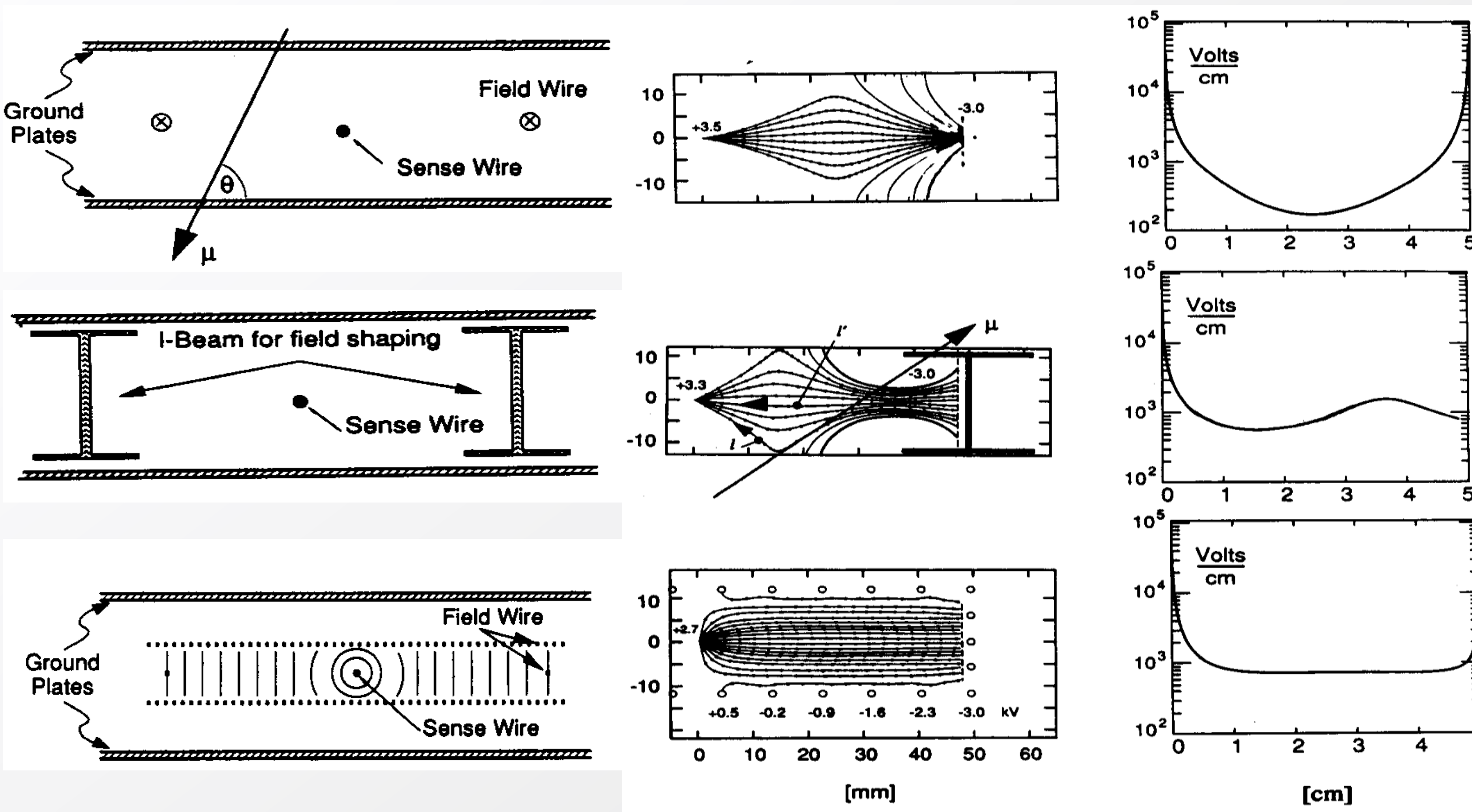

U. Becker in Instrumentation in High Energy Physics, World Scientific

Drift in Presence of E and B Fields

Equation of motion of free charge carriers in presence of E and B fields:

$$m\frac{d\vec{v}}{dt} = e\vec{E} + e(\vec{v}\times\vec{B}) + \vec{Q}(t)$$ where $\vec{Q}(t)$ stochastic force resulting from collisions

Time averaged solutions with assumptions: $\vec{v}_D = \langle \vec{v} \rangle = const.$; $<\vec{Q}(t)> = \frac{m}{\tau}\vec{v}_D$ friction force

$$\left\langle \frac{d\vec{v}}{dt} \right\rangle = 0 = e\vec{E} + e(\vec{v}_D\times\vec{B}) - \frac{m}{\tau}\vec{v}_D$$ τ mean time between collisions

$$\vec{v}_D = \frac{\mu|\vec{E}|}{1+\omega^2\tau^2}\left[\hat{E} + \omega\tau(\hat{E}\times\hat{B}) + \omega^2\tau^2(\hat{E}\cdot\hat{B})\hat{B}\right]$$

$\mu = \frac{e\tau}{m}$ mobility $\qquad \omega = \frac{eB}{m}$ cyclotron frequency

In general drift velocity has 3 components: $\| \vec{E}; \| \vec{B}; \| \vec{E}\times\vec{B}$

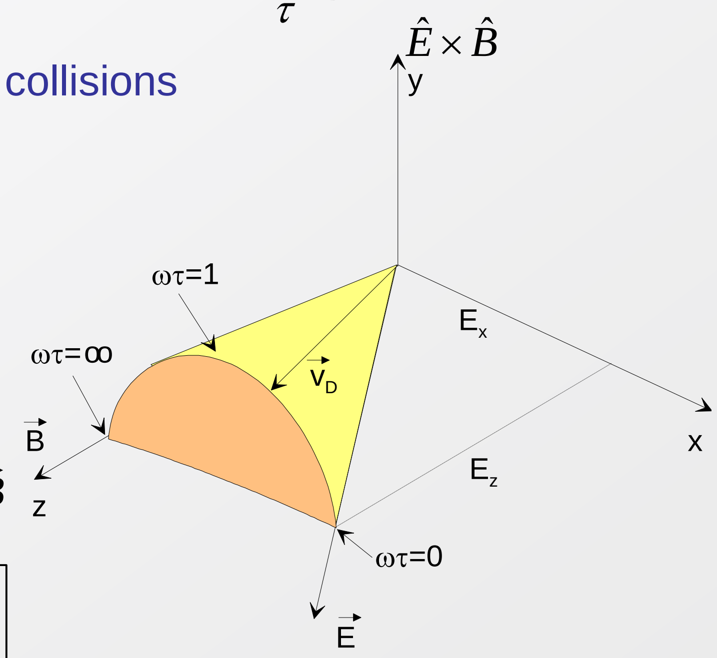

$B=0 \rightarrow \vec{v}_D^B = \vec{v}_D^0 = \mu\vec{E}$

$\vec{E} \| \vec{B} \rightarrow v_D^B = v_D^0$

$\vec{E} \perp \vec{B} \rightarrow v_D^B = \frac{E}{B}\frac{\omega\tau}{\sqrt{1+\omega^2\tau^2}}$

$\vec{E} \perp \vec{B}$

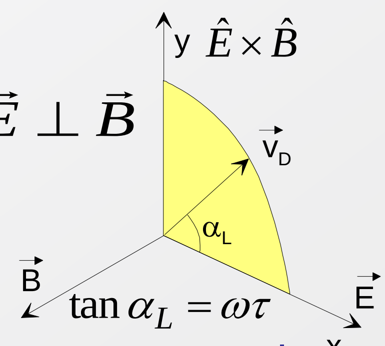

$\tan\alpha_L = \omega\tau$

Lorentz angle

$\omega\tau << 1$ particles follow E-field

$\omega\tau >> 1$ particles follow B-field

Diffusion Magnetic Anisotropy

$\vec{E} \parallel \vec{B}$

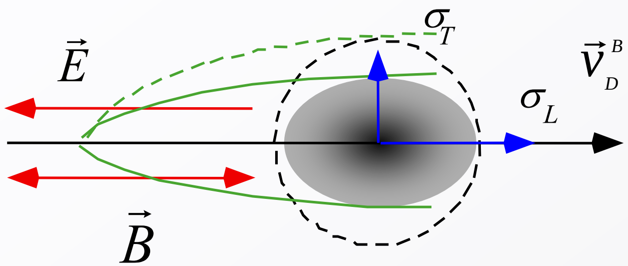

$$\sigma_L = \sigma_0$$

$$\sigma_T = \frac{\sigma_0}{\sqrt{1+\omega^2\tau^2}}$$

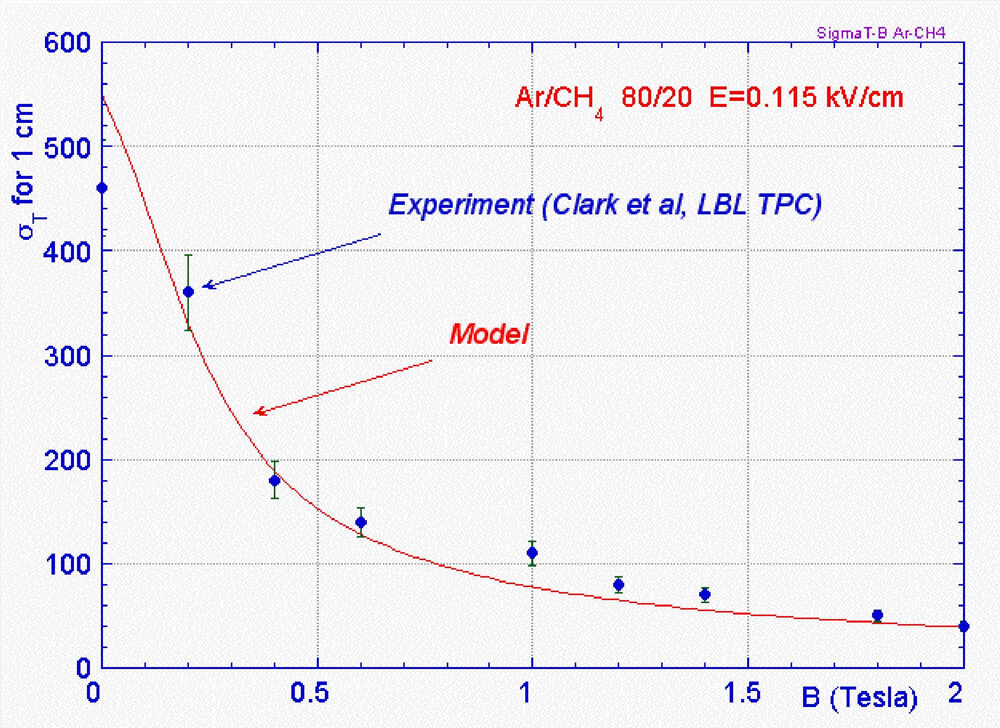

F. Sauli, IEEE Short Course on Radiation Detection and Measurement, Norfolk (Virginia) November 10-11, 2002

TPC – Time Projection Chamber

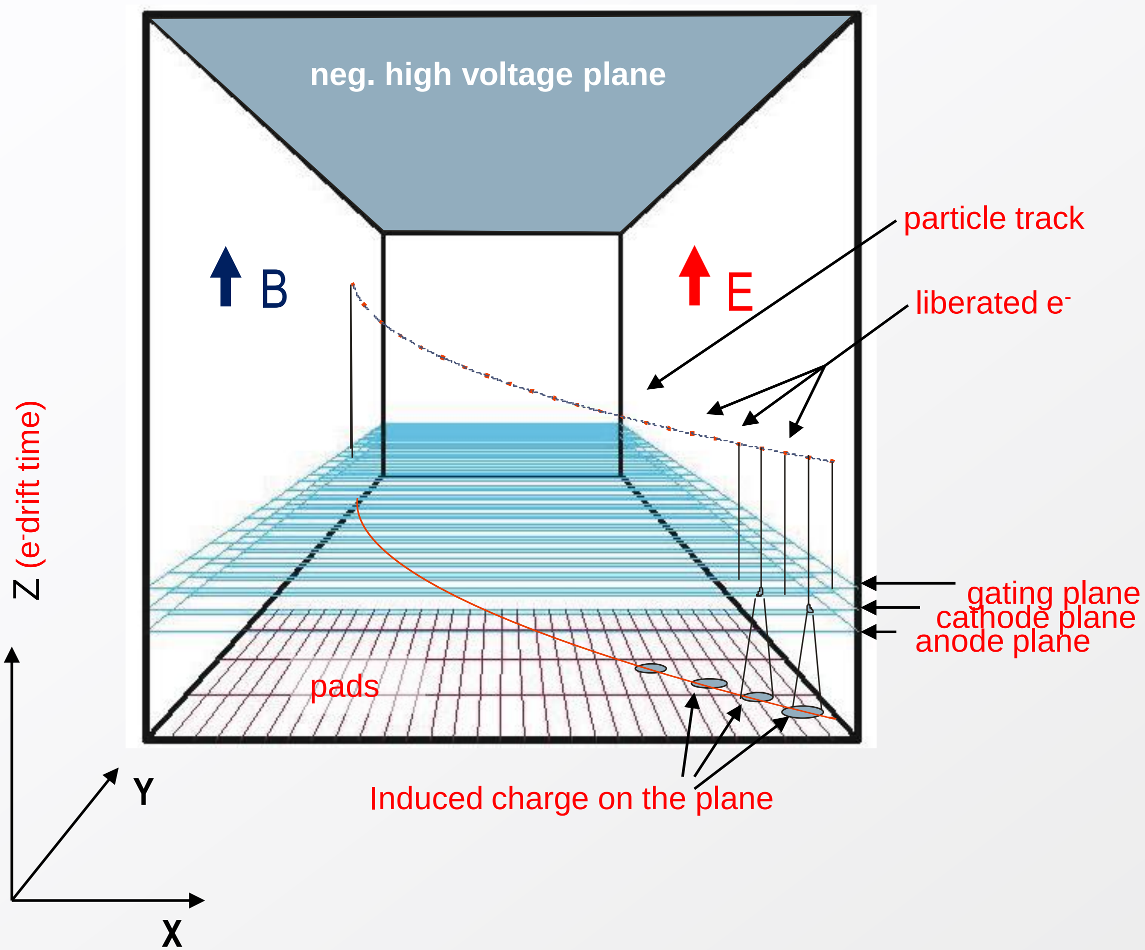

Time Projection Chamber

full 3D track reconstruction:

x-y from wires and segmented cathode of MWPC (or GEM)

z from drift time

- momentum resolution
  space resolution + B field
  (multiple scattering)
- energy resolution
  measure of primary ionization

TPC – Time Projection Chamber

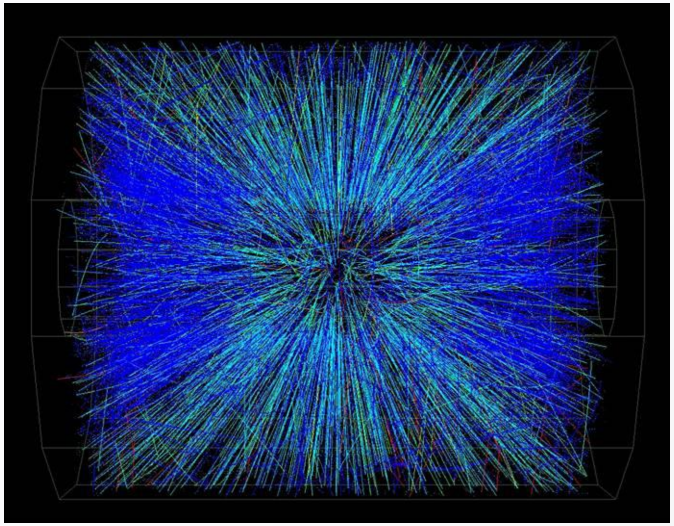

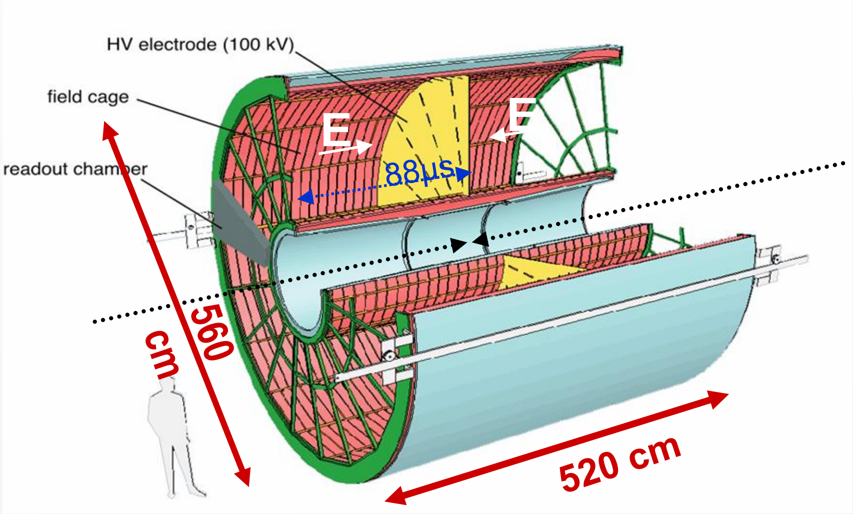

Alice TPC

HV central electrode at –100 kV

Drift length 250 cm at E = 400 V/cm

Gas Ne-CO_2 90-10

Space point resolution ~500 μm

dp/p = 2%@1GeV/c; 10%@10 GeV/c

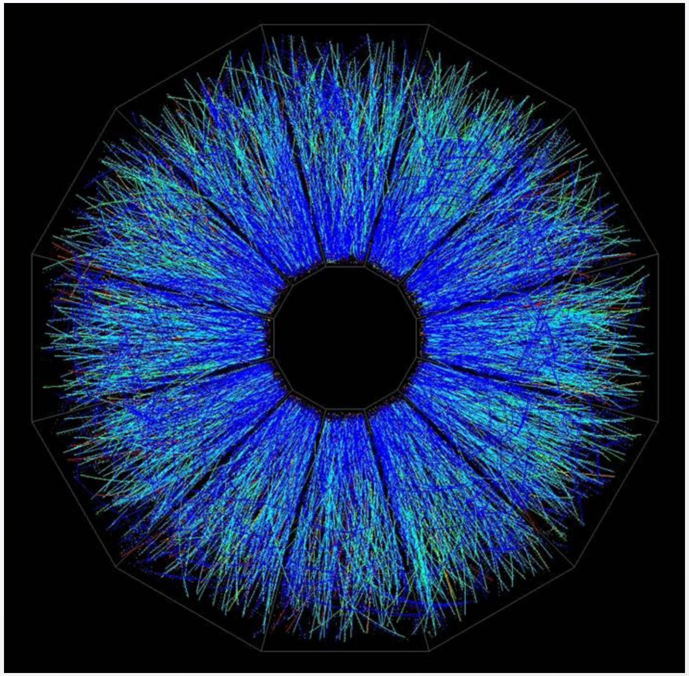

Events from STAR TPC at RHIC

Au-Au collisions at CM energy of 130 GeV/n

Typically ~2000 tracks/event

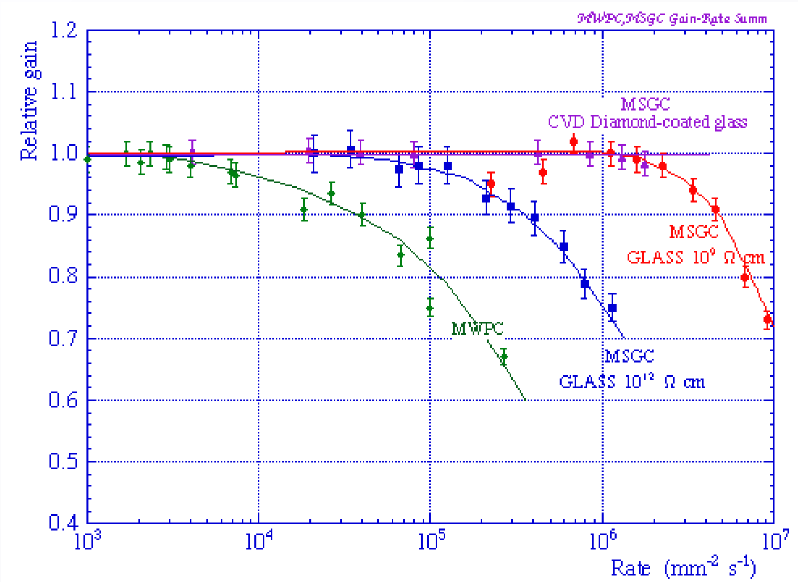

scale factor

1

5

10

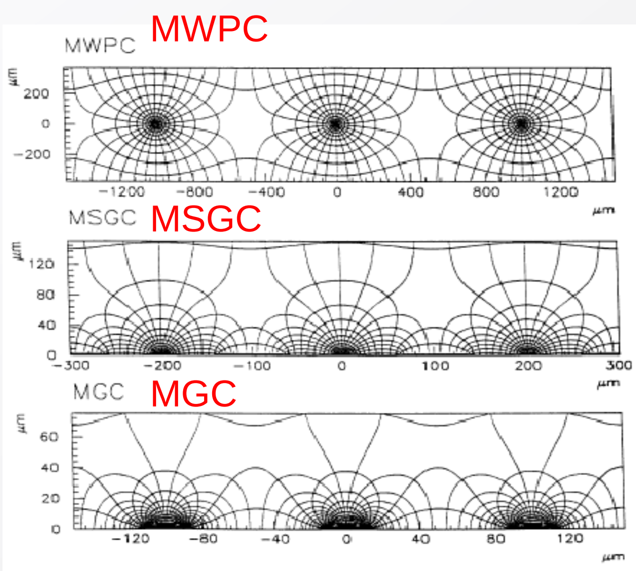

R. Bellazzini et al.

General advantages of gas detectors:

- low mass (in terms of radiation length)
- large areas at low price
- flexible geometry
- spatial, energy resolution …

Main limitation:

- rate capability limited by space charge defined by the time of evacuation of positive ions

Solution:

- reduction of the size of the detecting cell (limitation of the length of the ion path) using chemical etching techniques developed for microelectronics and keeping at same time similar field shape.

Micromegas – Micromesh Gaseous Structure

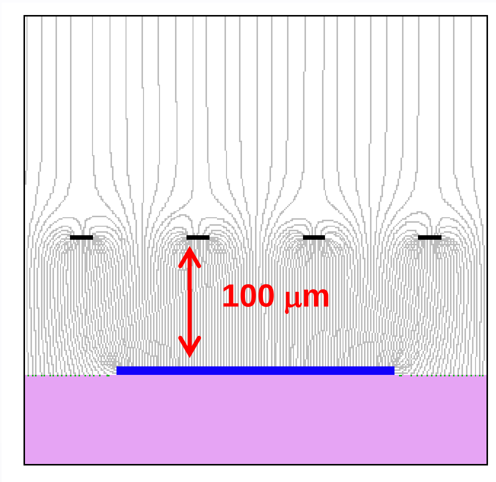

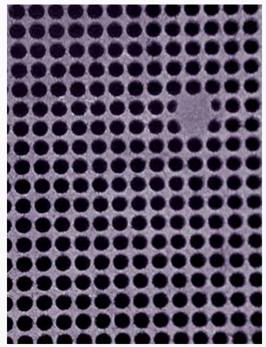

micromesh

Metal micromesh mounted above readout structure (typically strips).

E field similar to parallel plate detector.

E_a/E_i ~ 50 to ensure electron transparency and positive ion flowback supression.

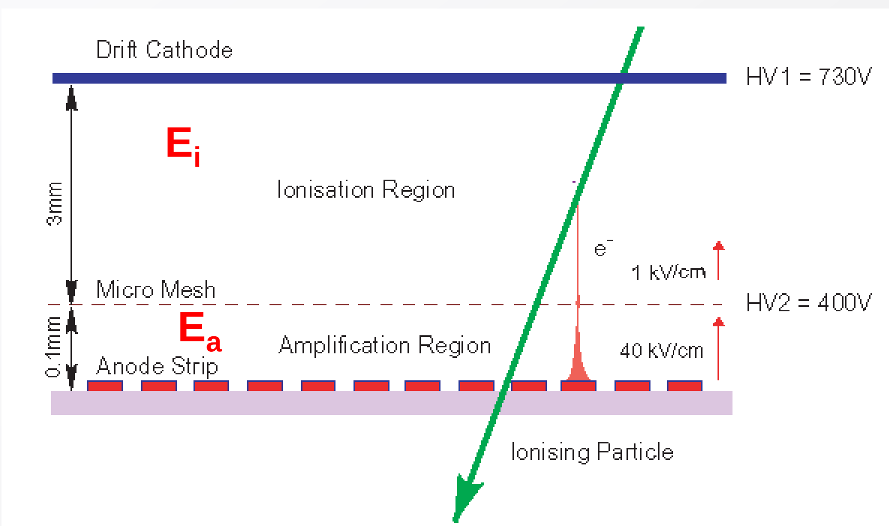

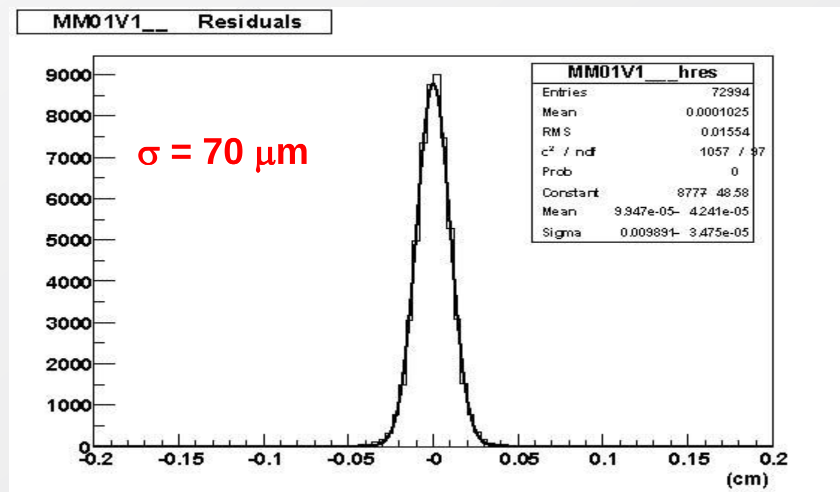

Space resolution

GEM – Gas Electron Multiplier

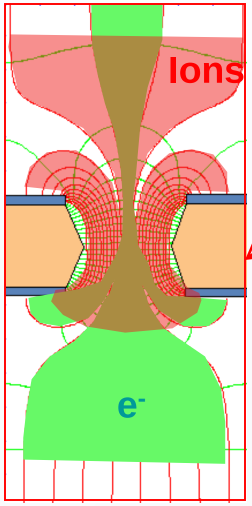

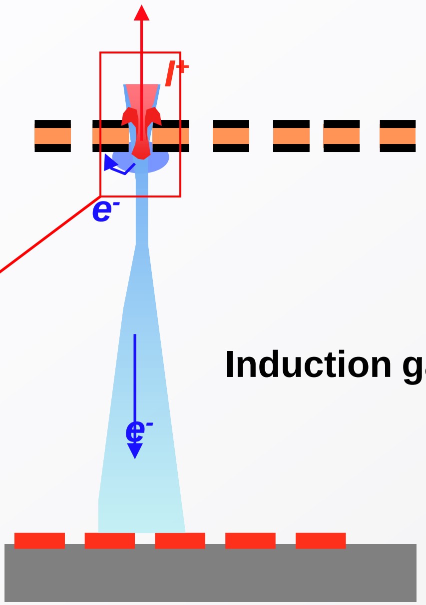

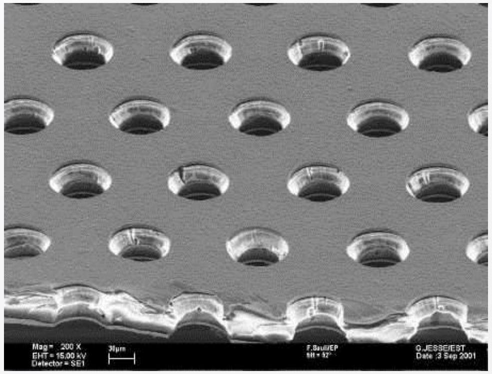

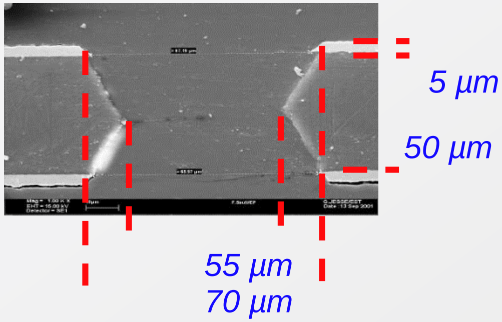

Thin, metal coated polyimide foil perforated with high density holes.

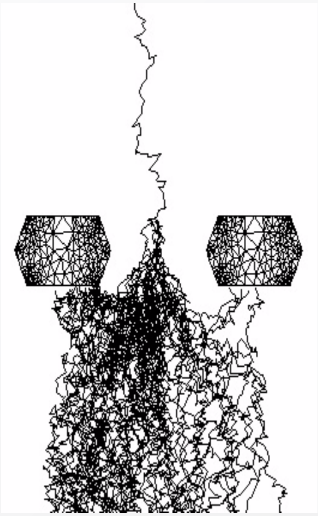

Electrons are collected on patterned readout board.
A fast signal can be detected on the lower GEM electrode for triggering or energy discrimination.
All readout electrodes are at ground potential.
Positive ions partially collected on the GEM electrodes.

GEM – Gas Electron Multiplier

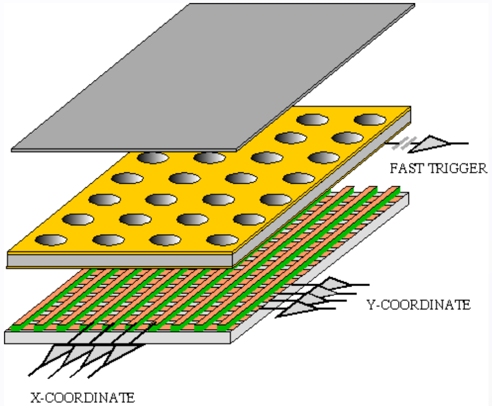

Full decupling of the charge ampification structure from the charge collection and readout structure.

Both structures can be optimized independently !

A. Bressan et al, Nucl. Instr. and Meth. A425(1999)254

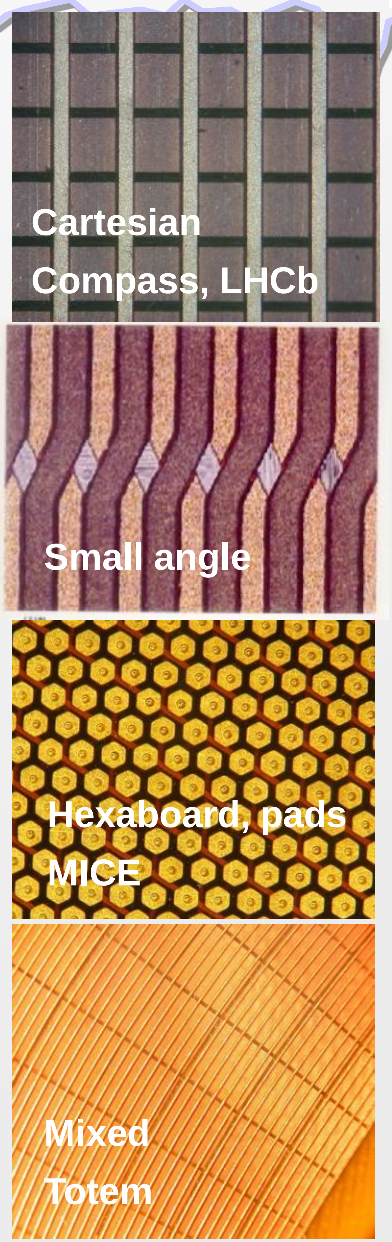

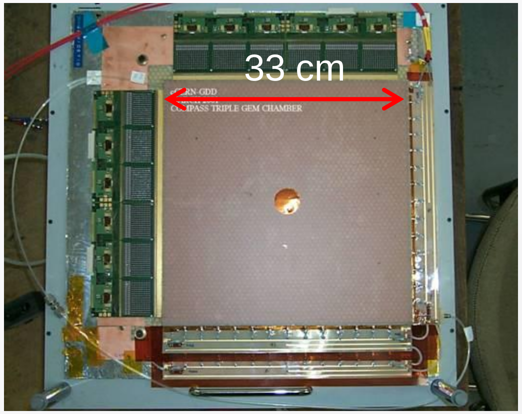

Compass

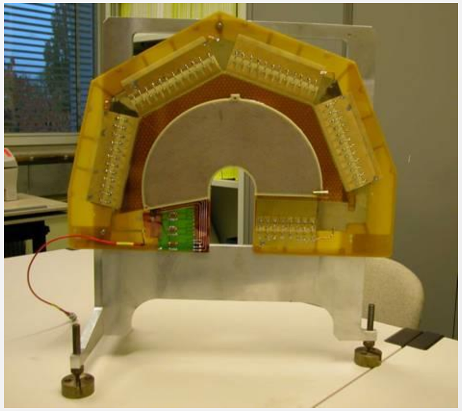

Totem

Both detectors use three GEM foils in cascade for amplification to reduce discharge probability by reducing field strenght.

TPC – Time Projection Chamber

extra slide not shown

Positive ion backflow modifies electric field resulting in track distortion.

Solution : gating

Prevents electrons to enter amplification region in case of uninteresting event;

Prevents ions created in avalanches to flow back to drift region.

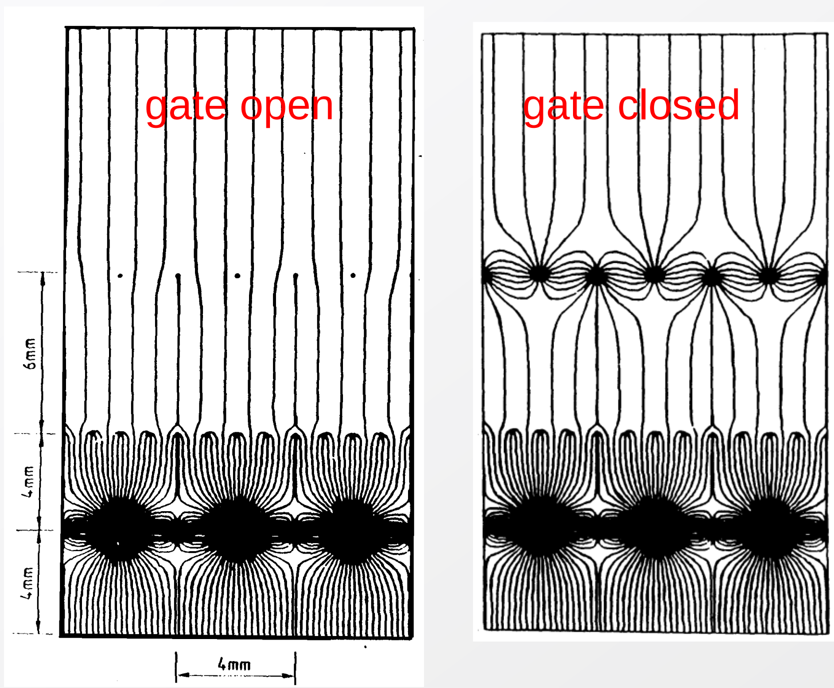

gating plane

cathode plane

anode wires

readout pads

ALEPH coll., NIM A294(1990)121

GEM – Gas Electron Multiplier

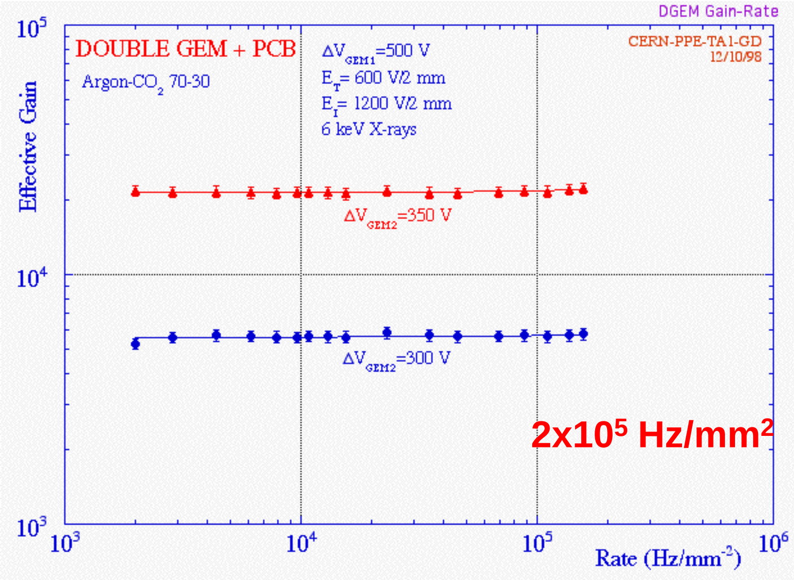

Rate capability

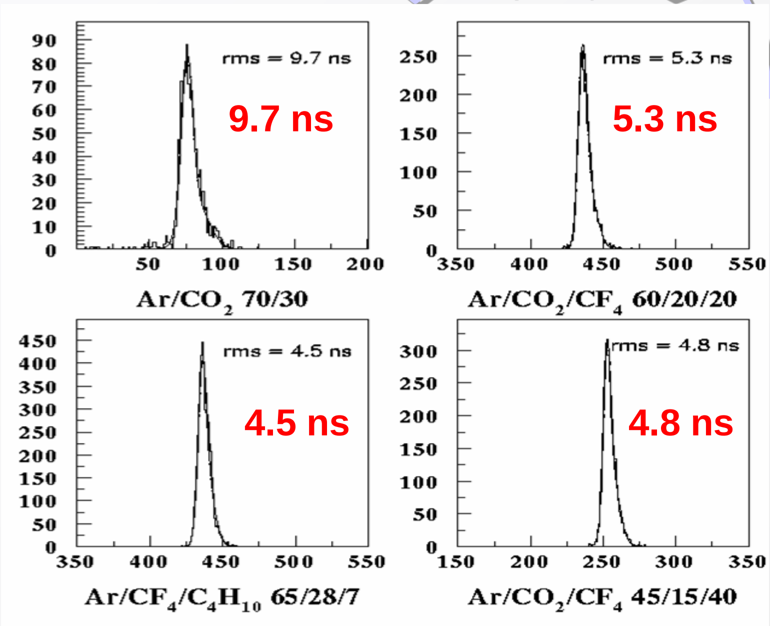

Time resolution

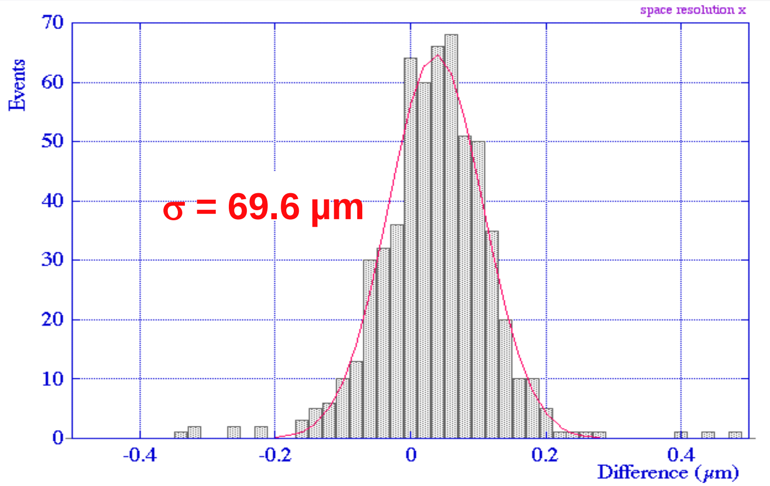

Space resolution

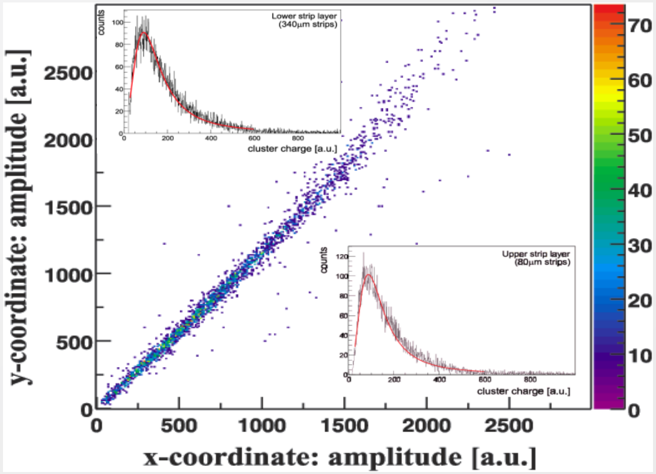

Charge corellation (cartesian readout)

Limitations of Gas Detectors

Classical ageing

Avalanche region → plasma formation (complicated plasma chemistry)

- Dissociation of detector gas and pollutants
- Highly active radicals formation
- Polymerization (organic quenchers)
- Insulating deposits on anodes and cathodes

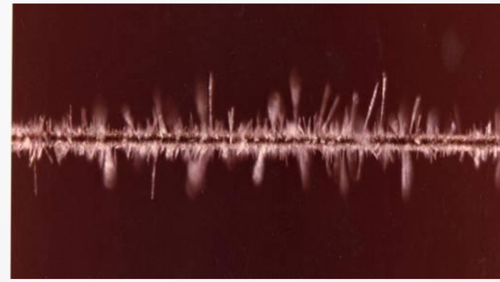
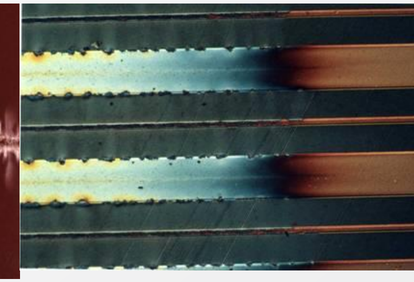

Anode: increase of the wire diameter, reduced and variable field, variable gain and energy resolution.

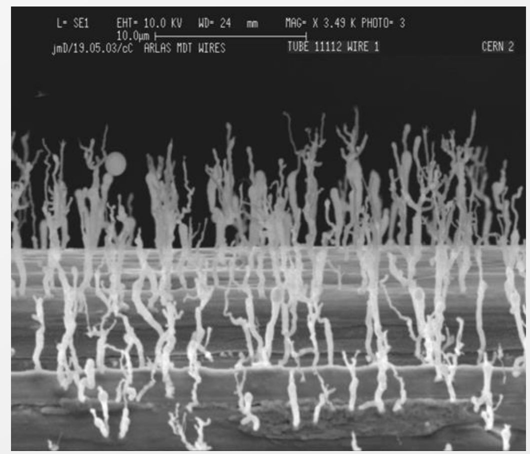
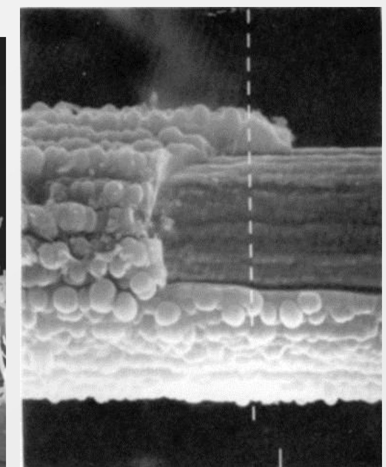

Cathode: formation of strong dipoles, field emmision and microdischarges (Malter effect).

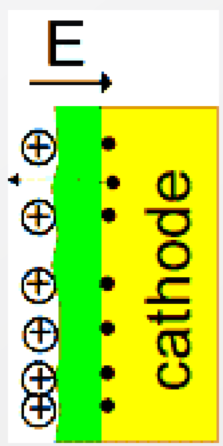

Limitations of Gas Detectors

Solutions: carefull material selection for the detector construction and gas system, detector type (GEM is resitant to classical ageing), working point, non-polymerizing gases, additives supressing polymerization (alkohols, methylal), additives increasing surface conductivity (H_2O vapour), clening additives (CF_4).

Discharges

Field and charge density dependent effect.

Solution: multistep amplification

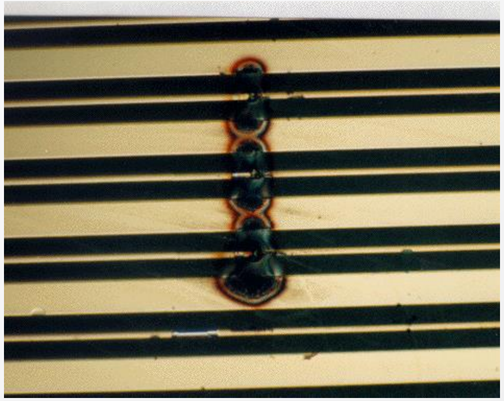

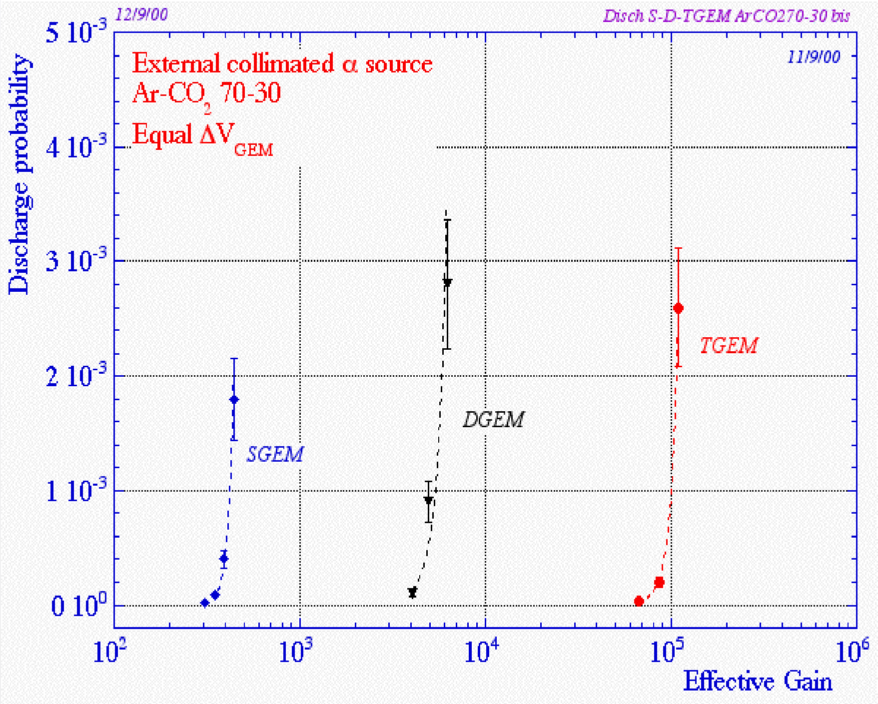

Space charge limiting rate capability

Solution: reduction of the lenght of the positive ion path

Insulator charging up resulting in gain variable with time and rate

Solution: slightly conductive materials